

Response theory for time-resolved second-harmonic generation and two-photon photoemission: Dependence on the pulse shape of the exciting light field

Carsten Timm* and K.H. Bennemann

Institut für Theoretische Physik, Freie Universität Berlin, Arnimallee 14, D-14195 Berlin, Germany

(February 27, 2001)

A unifying response theory for the time-resolved nonlinear light generation and two-photon photoemission (2PPE) from flat metal surfaces is presented. The theory describes the dependence of the nonlinear optical response and the photoelectron yield, respectively, on the pulse shape of the exciting laser. While our theory works for arbitrary pulse shapes, we mostly focus on the case of two pulses of the same mean frequency. The interplay between pulse shape, relaxation times of excited electrons, and band structure is analyzed directly in the time domain. The theory allows to discuss when the frequently used optical Bloch equations are valid and how collective excitations affect the nonlinear optical response and 2PPE.

I. INTRODUCTION

During the last decade time-resolved spectroscopy of condensed-matter systems has become a very active area of experimental research [1–17]. This is mainly due to the progress in experimental technique, in particular the ability to create ultra-short laser pulses with a duration of the order of a few femtoseconds [18]. Since this is similar to the relaxation times of excited electrons and collective excitations in solids, these experiments allow to study non-equilibrium physics, *e.g.*, the time evolution of excited electrons before and during thermalization. Of particular interest are non-linear techniques such as time-resolved sum-frequency generation (SFG) and two-photon photoemission (2PPE), which are sensitive to excited electron states [19]. A theoretical understanding of these processes is crucial. Petek and Ogawa [17] noted in 1997 that a theory for time-resolved 2PPE is still lacking, and, despite the efforts of many theorists, much remains to be done. The situation for SFG is similar. The construction of such a theory is a formidable task—the main problems are (a) the description of the time-dependent response and (b) the treatment of the surface. Our main concern here is the first point, while we treat the surface in a simplified manner using Fresnel formulas for the incoming light and related expressions for the outgoing field. This approach has been used rather successfully to describe SFG from metals [20–23].

In the present paper we discuss the electronic processes taking place during time-resolved SFG and 2PPE and derive the dependence of the SFG light intensity and the 2PPE photoelectron yield on the laser pulse shape. We show that most effects observed for time-resolved 2PPE appear similarly for SFG, such as their dependence on energy relaxation, dephasing, and detuning of intermediate states. Other examples are the enhancement of the response due to collective excitations and the sensitivity regarding the ultra-fast magnetic, spin-dependent relaxation. We also discuss the information that can be gained from performing simultaneously time-resolved SFG and 2PPE experiments. We develop a unifying time-dependent response theory for SFG and 2PPE, starting from the self-consistent field approach of Ehrenreich and Cohen [24,25], which is applied to metals described by their band structure, relaxation rates, and dipole matrix elements. For illustration, we apply the theory to a generic model consisting of a number of tight-binding bands to study interference effects in both pump-probe single-color SFG and 2PPE and their dependence on relaxation rates and detuning.

In SFG [1–5] electrons are excited by absorbing two photons and they subsequently emit a single photon at the sum frequency. Time-resolved SFG experiments have been performed less often than 2PPE. In Fig. 1 we illustrate the processes yielding SFG and the accompanying difference-frequency generation (DFG). For simplicity, we only talk about SFG in the following, although DFG is always included in our theory, as shown below. The experiments [1–5] usually employ the pump-probe technique, where two laser pulses of the same (single-color) or different (two-color) frequency are applied with a time delay ΔT between them. This time delay controls the time between the two absorptions and thus the relaxation dynamics of the electron in the intermediate state [2] is crucial, see Fig. 1. SFG

*Electronic address: timm@physik.fu-berlin.de.

is strongly surface-sensitive, since the SFG response of the bulk of an inversion-symmetric crystal vanishes in the dipole approximation. The most important case of SFG is second-harmonic generation (SHG), where the electrons are excited by approximately monochromatic light of frequency ω and light of frequency 2ω is detected. Note, in the case of ultra-short laser pulses the spectrum is necessarily broadened and a full treatment of SFG is required even for these single-color experiments.

Time-resolved 2PPE studies of metal surfaces [6–15] as well as of clusters [16] also employ the pump-probe technique. A review can be found in Ref. [17]. Figure 2 shows a sketch of the processes yielding 2PPE. An electron is excited above the vacuum energy E_{vac} due to the absorption of two photons. The interplay between the relaxation of the electrons in intermediate states and the time between the two absorptions will determine the resulting photoelectron current. The probability of electrons above the vacuum level actually leaving the solid is also crucial. The limited mean free path of the electrons makes photoemission surface-sensitive. In both SFG and 2PPE interference effects [1,3,8,11–13] appear, which our theory allows to study.

The response theory presented here goes beyond previous theoretical treatments of ultra-fast processes [26] in SFG and 2PPE in metals, which mainly fall into four classes: (a) density functional theory and approaches based thereon [27,28,23,29–32], (b) rate equations [15,33,34], (c) optical Bloch equations [9,12,35], and (d) perturbative methods [36]. At first, density functional theory has been applied in the time-dependent local-density approximation for jellium models [27–30]. In the jellium approximation one ignores the potential of the ion cores and, consequently, any band-structure effects. Thus this approach is not suitable if single bands or surface states are important. On the other hand, collective excitations are usually described rather well [37]. Going beyond the jellium model, Luce and Bennemann have employed the local density approximation to calculate dipole matrix elements as they enter also in our approach [23]. Additionally taking excited states into account within the *GW* approximation, Schöne *et al.* [31] have calculated electronic lifetimes. Hole dynamics have also been studied with density functional methods that include the real band structure [32].

However, one would like to gain more physical insight than the numerical results can provide. To this end one may consider rate equations for the occupation of excited states, *e.g.*, the Boltzmann equation [15,33,34]. In the Boltzmann equation one typically averages over the whole Brillouin zone (random- \mathbf{k} approximation). This approach allows to incorporate important effects such as secondary electrons due to relaxation from higher-energy states and to Auger processes as well as transport into the bulk [15,33,34]. However, rate equations neglect the electric polarization of the electron gas, its dephasing, and any quantum-mechanical interference effects. To include these effects one has to solve the equation of motion for the entire density matrix ρ , not only for its diagonal components referring to the occupations. This can be done in response theory. Its simplest form yields the optical Bloch equations: The metal is modelled by a small number of levels and the Liouville equation of motion (master equation) for the density matrix is integrated numerically [35,9,12]. However, this approach is in practice limited to a small number of levels so that a realistic band structure cannot be described. Furthermore, many-particle effects like collective excitations are not included.

On the other hand, the response theory presented here does include the band structure and collective excitations. It generalizes the theory of Hübner and Bennemann [25] to incorporate SFG due to incident light of arbitrary time dependence and spectrum. The previous theory [25] has been used successfully for SHG from metal surfaces, thin films, and quantum wells due to *continuous-wave*, monochromatic light [25,21–23,38–40]. However, it does not allow to discuss the dependence of SHG on the pulse shape and the effect of energy relaxation and dephasing. We also derive the response expressions for time-dependent 2PPE within the same framework. Our theory employs a generalized self-consistent-field approach [24,25], which is equivalent to the random-phase approximation (RPA) [41]. Note, the RPA is rather successful in deriving the dispersion and lifetime of bulk and surface plasmons [41–45], which is desirable for a description of SFG and 2PPE. We employ the electric-dipole approximation, which is valid for small wave vector \mathbf{q} of the electromagnetic field and has been used successfully to describe SHG from metal surfaces [21–23,38–40,46]. This is reasonable, since the skin depth, which is the length scale of field changes, is about one order of magnitude larger than the lattice constant. One has to take care in interpreting SFG experiments for inversion-symmetric crystals, since the surface contribution only dominates over higher multipole bulk contributions for surfaces of low symmetry [21,25]. Similar in spirit to our response theory, Ueba [47] has studied continuous-wave 2PPE and Shahbazyan and Perakis [36] have developed a time-dependent, but *linear* response theory for metallic nanoparticles.

The organization of the remainder of this paper is as follows: We first summarize the response theory for SFG and 2PPE in Sec. II. This lays the ground for our discussion in Sec. III of time-dependent SFG and 2PPE. Details of the response theory are given in appendices A and B. Boundary conditions and Fresnel factors are briefly reviewed in App. C, while further remarks on how plasmons enter in the response theory are made in App. D.

II. RESPONSE THEORY

A. Sum-frequency generation

We first outline the response theory for SFG. We consider a semi-infinite solid with single-particle states $|\mathbf{k}_\parallel l\rangle$ described by the momentum \mathbf{k}_\parallel parallel to the surface, which is assumed to be perpendicular to the z direction, and a set of additional quantum numbers l . For bulk states, which may be affected by the surface but are not localized close to it, the composite band index is $l = (k_z, \nu, \sigma)$, where k_z is the z momentum component in the bulk, ν is a band index, and σ is the spin quantum number. k_z has a continuous spectrum. On the other hand, for states localized at the surface, l is discrete (and also includes the spin σ). Examples are image-potential states, adsorbate states, quantum-well states in a thin overlayer, and proper surface states. The single-particle energies form a band structure $E_{\mathbf{k}_\parallel l}$.

Part of the electron-electron interaction is included by the self-consistent-field approximation or RPA [24,41]. The remaining electron-electron scattering is approximately taken into account by inserting phenomenological relaxation rates [48] into the single-electron Green functions and by shifting the band energies $E_{\mathbf{k}_\parallel l}$ [49]. We assume that $E_{\mathbf{k}_\parallel l}$ are quasiparticle energies containing all shifts. Note, the electron-phonon interaction only becomes relevant on longer time scales and is not considered here [26].

The electrons are coupled to the effective electric field \mathbf{E} within the solid through a dipolar interaction term. The optically induced polarization \mathbf{P} within the solid is expanded in orders of the electric field \mathbf{E} . The *linear* response is given by

$$P_i^{(1)}(\mathbf{q}, t) = \frac{1}{2\pi} \sum_{q_z} \int dt' \chi_{ij}(\mathbf{q}, \mathbf{q}'; t - t') E_j(\mathbf{q}', t'), \quad (1)$$

where χ_{ij} is the linear susceptibility, and $\mathbf{q}_\parallel = \mathbf{q}'_\parallel$ due to conservation of momentum parallel to the surface. Summation over repeated indices is always implied. The non-conservation of q_z is explicitly taken into account here. The self-consistent-field approach gives

$$\begin{aligned} \chi_{ij}(\mathbf{q}, \mathbf{q}'; t - t') &= \frac{e^2}{V} \frac{2\pi i}{\hbar} \Theta(t - t') \\ &\times \sum_{\mathbf{k}_\parallel} \sum_{ll'} D_{\mathbf{k}_\parallel + \mathbf{q}_\parallel, l'; \mathbf{k}_\parallel l}^i(-\mathbf{q}) D_{\mathbf{k}_\parallel l; \mathbf{k}_\parallel + \mathbf{q}_\parallel, l'}^j(\mathbf{q}') \\ &\times [f(E_{\mathbf{k}_\parallel l'}) - f(E_{\mathbf{k}_\parallel l})] \exp\left[i \frac{E_{\mathbf{k}_\parallel l'} - E_{\mathbf{k}_\parallel l}}{\hbar} (t - t')\right] \\ &\times \exp[-\Gamma_{\mathbf{k}_\parallel l; \mathbf{k}_\parallel l'} (t - t')], \end{aligned} \quad (2)$$

where V is the volume of the system. We have suppressed the small \mathbf{q}_\parallel in the band energies and relaxation rates for clarity. The dipole matrix elements are

$$\mathbf{D}_{\mathbf{k}_\parallel l; \mathbf{k}'_\parallel l'}(\mathbf{q}) \equiv \langle \mathbf{k}_\parallel l | \mathbf{r} e^{-i\mathbf{q} \cdot \mathbf{r}} | \mathbf{k}'_\parallel l' \rangle. \quad (3)$$

The linear susceptibility is represented by the usual Feynman diagram shown in Fig. 3 [50].

The finite lifetime of electrons due to their interaction enters Eq. (2) through the *dephasing* rates $\Gamma_{\mathbf{k}_\parallel l; \mathbf{k}'_\parallel l'}$, which describe the decay of the polarization due to the superposition of states $|\mathbf{k}_\parallel l\rangle$ and $|\mathbf{k}'_\parallel l'\rangle$. The change of the occupation of states is described by the *energy relaxation* rates $\Gamma_{\mathbf{k}_\parallel l; \mathbf{k}_\parallel l} \equiv \tau_{\mathbf{k}_\parallel l}^{-1}$, where $\tau_{\mathbf{k}_\parallel l}$ are the lifetimes. $\Gamma_{\mathbf{k}_\parallel l; \mathbf{k}_\parallel l}$ is the rate of spontaneous transitions out of the state $|\mathbf{k}_\parallel l\rangle$. Since the depopulation of the states $|\mathbf{k}_\parallel l\rangle$ or $|\mathbf{k}'_\parallel l'\rangle$ certainly leads to the destruction of the polarization, the dephasing rates can be expressed in terms of the lifetimes as [49]

$$\Gamma_{\mathbf{k}_\parallel l; \mathbf{k}'_\parallel l'} = \frac{\tau_{\mathbf{k}_\parallel l}^{-1} + \tau_{\mathbf{k}'_\parallel l'}^{-1}}{2} + \Gamma_{\mathbf{k}_\parallel l; \mathbf{k}'_\parallel l'}^{\text{ph}}, \quad (4)$$

where Γ^{ph} describes additional dephasing.

The second-order polarization is given by

$$P_i^{(2)}(t) = \frac{1}{(2\pi)^2} \int dt_1 dt_2 \chi_{ijk}^{(2)}(t, t_1, t_2) E_j(t_1) E_k(t_2). \quad (5)$$

The second-order susceptibility $\chi^{(2)}$ depends only on two time differences due to homogeneity in time. To express the electric field \mathbf{E} within the solid in terms of the applied external light field \mathbf{E}_{las} and similarly the electric field \mathbf{E}_{out} of the outgoing light in terms of the polarization \mathbf{P} we use Fresnel formulas [20,21], which are summarized in App. C. The intensity of SFG light is $I^{(2)}(t) \propto [E_{\text{out}}^{(2)}(t)]^2$. Typical experiments so far do not resolve the time dependence of the intensity, but only measure the time-integrated SFG yield

$$\mathcal{I}^{(2)} \equiv \int dt I^{(2)}(t) \propto \int dt [E_{\text{out}}^{(2)}(t)]^2. \quad (6)$$

In pump-probe experiments the time resolution is achieved by measuring $\mathcal{I}^{(2)}(\Delta T)$ as a function of the time delay ΔT between the pulses. Omitting surface effects to emphasize the structure of the results, the yield can be written as

$$\begin{aligned} \mathcal{I}^{(2)}(\Delta T) &\propto \int dt dt_1 dt_2 dt_3 dt_4 \chi_{ijk}^{(2)}(t, t_1, t_2) \\ &\times \chi_{ilm}^{(2)}(t, t_3, t_4) E_j(t_1) E_k(t_2) E_l(t_3) E_m(t_4), \end{aligned} \quad (7)$$

which is of fourth order in the incoming light field and of second order in its intensity.

To understand that both SFG and DFG are included we write down the Fourier-transformed second-order polarization

$$P_i^{(2)}(\omega) = \int d\omega' \chi_{ijk}^{(2)}(\omega, \omega') E_j(\omega') E_k(\omega - \omega'), \quad (8)$$

where

$$\begin{aligned} \chi_{ijk}^{(2)}(t, t_1, t_2) &= \int d\omega d\omega' e^{-i\omega(t-t_2)} e^{-i\omega'(t_2-t_1)} \\ &\times \chi_{ijk}^{(2)}(\omega, \omega'). \end{aligned} \quad (9)$$

As illustrated in Fig. 1, Eq. (8) shows that $\mathbf{P}^{(2)}$ only has components at the *sum* of two frequencies of the incoming light. Since the Fourier transform of the electric field contains positive and negative frequencies, the difference frequency also appears.

If we ignore screening effects as a first step, Eqs. (5) and (7) only contain the second-order *irreducible* susceptibility derived in App. A,

$$\begin{aligned} \chi_{\text{irr};ijk}^{(2)}(\mathbf{q}, \mathbf{q}_1, \mathbf{q}_2; t, t_1, t_2) &= -\frac{e^3}{V} \left(\frac{2\pi i}{\hbar} \right)^2 \Theta(t - t_1) \Theta(t_1 - t_2) \sum_{\mathbf{k}_{\parallel}} \sum_{l'l''} D_{\mathbf{k}_{\parallel} + \mathbf{q}_{1\parallel}, l; \mathbf{k}_{\parallel} l''}^i(-\mathbf{q}) \left(D_{\mathbf{k}_{\parallel} l''; \mathbf{k}_{\parallel} + \mathbf{q}_{1\parallel}, l'}^j(\mathbf{q}_1) \right. \\ &\times D_{\mathbf{k}_{\parallel} + \mathbf{q}_{1\parallel}, l'; \mathbf{k}_{\parallel} + \mathbf{q}_{\parallel}, l}^k(\mathbf{q}_2) [f(E_{\mathbf{k}_{\parallel} l}) - f(E_{\mathbf{k}_{\parallel} l'})] \exp \left[i \frac{E_{\mathbf{k}_{\parallel} l} - E_{\mathbf{k}_{\parallel} l'}}{\hbar} (t_1 - t_2) \right] \exp[-\Gamma_{\mathbf{k}_{\parallel} l'; \mathbf{k}_{\parallel} l}(t_1 - t_2)] \\ &- D_{\mathbf{k}_{\parallel} + \mathbf{q}_{\parallel} - \mathbf{q}_{1\parallel}, l'; \mathbf{k}_{\parallel} + \mathbf{q}_{\parallel}, l}^j(\mathbf{q}_1) D_{\mathbf{k}_{\parallel} l''; \mathbf{k}_{\parallel} + \mathbf{q}_{\parallel} - \mathbf{q}_{1\parallel}, l'}^k(\mathbf{q}_2) [f(E_{\mathbf{k}_{\parallel} l'}) - f(E_{\mathbf{k}_{\parallel} l''})] \exp \left[i \frac{E_{\mathbf{k}_{\parallel} l'} - E_{\mathbf{k}_{\parallel} l''}}{\hbar} (t_1 - t_2) \right] \\ &\times \exp[-\Gamma_{\mathbf{k}_{\parallel} l''; \mathbf{k}_{\parallel} l'}(t_1 - t_2)] \left. \right) \exp \left[i \frac{E_{\mathbf{k}_{\parallel} l} - E_{\mathbf{k}_{\parallel} l''}}{\hbar} (t - t_1) \right] \exp[-\Gamma_{\mathbf{k}_{\parallel} l''; \mathbf{k}_{\parallel} l}(t - t_1)]. \end{aligned} \quad (10)$$

The terminology is explained below. We again neglect the photon momenta $\mathbf{q}_1, \mathbf{q}_2$ (incoming) and \mathbf{q} (outgoing), except in the matrix elements. This expression, which forms the basis of our discussion of SFG, goes beyond Ref. [25] in that it is valid for any time-dependent and spatially varying laser field. Furthermore, it includes the transverse response explicitly. Equation (10) already exhibits the interplay between the time passing between absorptions, the photon frequencies, the dephasing times, and the transition frequencies. Note, Fig. 1 suggests a simple picture of the optical excitation of electrons, which is often used in the literature: An electron is excited to an intermediate level by the absorption of a photon, from where it can either fall back with some relaxation rate Γ or be excited further by a second absorption. However, our result for $\chi_{\text{irr}}^{(2)}$ shows that a more careful discussion is needed: We consider the first of the two terms in Eq. (10), the second one is similar [51]. The gist of our arguments is illustrated in Fig. 4. The step functions incorporate the time ordering $t_2 < t_1 < t$ and thus guarantee causality. The system is in equilibrium until the first absorption at time t_2 creates a *superposition* of the two states $|\mathbf{k}_{\parallel} l\rangle$ and $|\mathbf{k}_{\parallel} l'\rangle$, denoted by the wavy

line in Fig. 4. The Fermi functions make sure that one of the states is initially occupied and the other is empty. Let us say state $|\mathbf{k}_{\parallel}l\rangle$ is occupied. Since the system is in a superposition of two eigenstates, the polarization oscillates with the transition frequency $(E_{\mathbf{k}_{\parallel}l} - E_{\mathbf{k}_{\parallel}l'})/\hbar$, expressed by the first exponential in the parentheses in Eq. (10). Such superpositions are described by the *off-diagonal* components of the density matrix [52]. The *diagonal* components denoting the occupation numbers of states are not changed by a single absorption. The superposition decays with the dephasing rate $\Gamma_{\mathbf{k}_{\parallel}l';\mathbf{k}_{\parallel}l}$ associated with this transition, making it clear why the dephasing rates rather than the energy relaxation rates dominate the response. A second absorption at the later time [53] t_1 changes the state into a superposition of the originally occupied state and the state $|\mathbf{k}_{\parallel}l''\rangle$ with its own characteristic oscillation frequency $(E_{\mathbf{k}_{\parallel}l} - E_{\mathbf{k}_{\parallel}l''})/\hbar$ and dephasing rate. This oscillating polarization can emit a photon at the frequency $(E_{\mathbf{k}_{\parallel}l} - E_{\mathbf{k}_{\parallel}l''})/\hbar$, after which the electron is again in the pure eigenstate $|\mathbf{k}_{\parallel}l\rangle$. The nonlinear susceptibility in Eq. (10) contains a sum over many contributions of this type from different momenta and bands. Note, the product of three dipole matrix elements appearing in $\chi_{\text{irr}}^{(2)}$ is responsible for the surface sensitivity of SFG.

The nonlinear susceptibility can also be written in frequency space,

$$\begin{aligned} \chi_{\text{irr};ijk}^{(2)}(\mathbf{q}, \mathbf{q}_1, \mathbf{q}_2; \omega, \omega') &= -\frac{e^3}{V} \sum_{\mathbf{k}_{\parallel}} \sum_{l'l''} \\ &\times \frac{D_{\mathbf{k}_{\parallel}+\mathbf{q}_{\parallel},l;\mathbf{k}_{\parallel}l''}^i(-\mathbf{q})}{-\hbar\omega + E_{\mathbf{k}_{\parallel}l} - E_{\mathbf{k}_{\parallel}l''} - i\hbar\Gamma_{\mathbf{k}_{\parallel}l'';\mathbf{k}_{\parallel}l}} \\ &\times \left[D_{\mathbf{k}_{\parallel}l'';\mathbf{k}_{\parallel}+\mathbf{q}_{\parallel},l'}^j(\mathbf{q}_1) D_{\mathbf{k}_{\parallel}+\mathbf{q}_{\parallel},l';\mathbf{k}_{\parallel}+\mathbf{q}_{\parallel},l}^k(\mathbf{q}_2) \right. \\ &\quad \times \frac{f(E_{\mathbf{k}_{\parallel}l}) - f(E_{\mathbf{k}_{\parallel}l'})}{-\hbar\omega + \hbar\omega' + E_{\mathbf{k}_{\parallel}l} - E_{\mathbf{k}_{\parallel}l'} - i\hbar\Gamma_{\mathbf{k}_{\parallel}l';\mathbf{k}_{\parallel}l}} \\ &\quad \left. - D_{\mathbf{k}_{\parallel}+\mathbf{q}_{\parallel}-\mathbf{q}_{\parallel},l';\mathbf{k}_{\parallel}+\mathbf{q}_{\parallel},l}^j(\mathbf{q}_1) D_{\mathbf{k}_{\parallel}l'';\mathbf{k}_{\parallel}+\mathbf{q}_{\parallel}-\mathbf{q}_{\parallel},l'}^k(\mathbf{q}_2) \right. \\ &\quad \left. \times \frac{f(E_{\mathbf{k}_{\parallel}l'}) - f(E_{\mathbf{k}_{\parallel}l''})}{-\hbar\omega + \hbar\omega' + E_{\mathbf{k}_{\parallel}l'} - E_{\mathbf{k}_{\parallel}l''} - i\hbar\Gamma_{\mathbf{k}_{\parallel}l'';\mathbf{k}_{\parallel}l'}} \right]. \end{aligned} \quad (11)$$

This shows that, since the intermediate states are virtual, the energy of the initial state plus the photon energy need not match the band energy of the intermediate state. Instead, their contribution is seen to fall off with the inverse of the detuning. Of course, this is due to Heisenberg's uncertainty principle, which allows energy conservation to be violated on short time scales, and is not related to the lifetime broadening.

So far, we have neglected the screening of the electric fields. Screening enters in two ways: First, the effective field \mathbf{E} within the solid is not identical to the external field because of the linear polarization of the solid. Secondly, the second-order polarization $\mathbf{P}^{(2)}$ of the electron gas, which corresponds to a displacement of charge, leads to the appearance of an additional electric field oscillating with the same frequency as $\mathbf{P}^{(2)}$. This electric field is given by

$$\mathbf{E}^{(2)}(\mathbf{k}, t) = -4\pi \hat{\mathbf{k}} \hat{\mathbf{k}} \cdot \mathbf{P}^{(2)}(\mathbf{k}, t), \quad (12)$$

where $\hat{\mathbf{k}}$ is the unit vector in the direction of \mathbf{k} . Only the longitudinal part of $\mathbf{P}^{(2)}$ is accompanied by an electric field, as discussed in App. A. This longitudinal polarization usually exists for transverse external fields due to the breaking of lattice symmetry by the surface. If $\mathbf{E}^{(2)}$ is taken into account selfconsistently the nonlinear susceptibility $\chi_{ijk}^{(2)}$ obtains an additional factor:

$$\begin{aligned} \chi_{ijk}^{(2)}(\mathbf{q}, \mathbf{q}_1, \mathbf{q}_2; t, t_1, t_2) &= \frac{1}{2\pi} \sum_m \sum_{\tilde{\mathbf{q}}} \int d\tilde{t} \\ &\times \varepsilon_{\text{long};im}^{-1}(\mathbf{q}, \tilde{\mathbf{q}}; t - \tilde{t}) \chi_{\text{irr};mjk}^{(2)}(\tilde{\mathbf{q}}, \mathbf{q}_1, \mathbf{q}_2; \tilde{t}, t_1, t_2), \end{aligned} \quad (13)$$

where the irreducible susceptibility $\chi_{\text{irr}}^{(2)}$ is given by Eq. (10). Here, $\varepsilon_{\text{long};ij}(\mathbf{q}, \tilde{\mathbf{q}}; t - \tilde{t}) \equiv \varepsilon_{im}(\mathbf{q}, \tilde{\mathbf{q}}; t - \tilde{t}) \hat{q}_m \hat{q}_j$ and $\varepsilon = 1 + 4\pi\chi$ is the dielectric tensor with the linear susceptibility of Eq. (2). $\varepsilon_{\text{long}}$ only acts on the longitudinal component. $\varepsilon_{\text{long};im}^{-1}(\mathbf{q}, \tilde{\mathbf{q}}; t - \tilde{t})$ is the inverse matrix with respect to the indices (i, q_z) and (m, \tilde{q}_z) .

Figure 5(a) shows the diagram of the second-order susceptibility $\chi^{(2)}$. The square vertex represents the additional factor of $\varepsilon_{\text{long}}^{-1}$. It is obtained from the Dyson equation in Fig. 5(b). The expression for $\chi_{\text{irr}}^{(2)}$ in Eq. (10) is called irreducible, since its diagram Fig. 5(a) with the square vertex replaced by a normal one cannot be cut into two by severing a single photon line.

The response theory we have developed clarifies how collective plasma excitations affect SFG, as we discuss briefly in the following. Additional remarks are made in App. D. Bulk plasmons essentially enter in two ways, both of which are controlled by the dielectric function ε : First, the effective electric field is expressed in terms of the external field by means of Fresnel formulas, which contain contributions of order $1/n^2 = 1/\varepsilon$ for small ε , where n is the refractive index, see Eq. (C1) in App. C. In our approach $\varepsilon = 1 + 4\pi\chi$ is determined by Eq. (2). Since our approach goes beyond the RPA by incorporating relaxation rates, it should give better results for plasmon lifetimes [54]. The dielectric function ε becomes small at the bulk plasmon resonance, since the photon momentum is small. This contribution is purely an effect of *field enhancement*. The outgoing (sum-frequency) electric field \mathbf{E}_{out} also contains terms that are *enhanced* for small ε , as shown by Eqs. (C4)–(C7).

Secondly, the nonlinear polarization $\mathbf{P}^{(2)}$ of the electron system is accompanied by an electric field $\mathbf{E}^{(2)}$, given in Eq. (12). This effect is responsible for the appearance of the factor $\varepsilon_{\text{long}}^{-1}$ in the nonlinear susceptibility in Eq. (13) [25]. This corresponds to an enhancement of the SFG light if ε is small, *i.e.*, if the *sum frequency* is close to the plasmon frequency.

B. Two-photon photoemission

To demonstrate the similarities between SFG and 2PPE, we continue by summarizing the results of the response theory for 2PPE. We consider the same band structure as for SFG, which is characterized by single-electron energies $E_{\mathbf{k}_{\parallel}l}$. We emphasize that this band structure contains the bulk states with the z -component k_z of \mathbf{k} included in l .

The response theory starts from the observation that the photoelectron current $j(t; \mathbf{k}, \sigma)$ of electrons of momentum \mathbf{k} and spin σ is given by the change of occupation of the vacuum state $|\mathbf{k}\sigma, \text{out}\rangle$ outside of the crystal. However, in practice the time-dependence of j is not measured but only the total photoelectron yield $\mathcal{N}(\mathbf{k}, \sigma) = \int dt j(t; \mathbf{k}, \sigma)$. This is similar to SFG, where only the time-integrated intensity is measured. The response theory directly determines the photoelectron yield \mathcal{N} . To prepare the discussion it is useful to first consider ordinary, single-photon photoemission. The yield of single-photon photoemission is given by

$$\begin{aligned} \mathcal{N}^{(2)}(\mathbf{k}, \sigma) &= \sum_{\mathbf{q}} \int dt_1 dt_2 E_i(\mathbf{q}, t_1) \eta_{ij}^{(2)}(\mathbf{q}; t_1, t_2; \mathbf{k}, \sigma) \\ &\quad \times E_j(-\mathbf{q}, t_2), \end{aligned} \quad (14)$$

with the response function (see App. B)

$$\begin{aligned} \eta_{ij}^{(2)}(\mathbf{q}; t_1, t_2; \mathbf{k}, \sigma) &= \frac{e^2}{\hbar^2} \frac{\gamma_{\mathbf{k}\sigma, \text{out}; \mathbf{k}\sigma, \text{in}}}{\Gamma_{\mathbf{k}\sigma, \text{in}; \mathbf{k}\sigma, \text{in}}} \sum_{\lambda} D_{\mathbf{k}\sigma, \text{in}; \mathbf{k}_{\parallel} + \mathbf{q}_{\parallel}, \lambda}^i(\mathbf{q}) \\ &\quad \times \exp \left[i \frac{E_{\mathbf{k}_{\parallel} \lambda} - E_{\mathbf{k}\sigma, \text{in}}}{\hbar} (t_2 - t_1) \right] e^{-\Gamma_{\mathbf{k}_{\parallel} \lambda; \mathbf{k}\sigma, \text{in}} |t_2 - t_1|} \\ &\quad \times f(E_{\mathbf{k}_{\parallel} \lambda}) D_{\mathbf{k}_{\parallel} + \mathbf{q}_{\parallel}, \lambda; \mathbf{k}\sigma, \text{in}}^j(-\mathbf{q}). \end{aligned} \quad (15)$$

We have again neglected the momentum transferred by the photon. The yield is proportional to the intensity of incoming light. The standard diagrammatic representation of ordinary photoemission is shown in Fig. 6 [55]. The effective field \mathbf{E} within the solid is again expressed in terms of the external light field with the help of the proper boundary conditions, see App. C. The response function $\eta^{(2)}$ will play a role when we discuss the various contributions to 2PPE.

We briefly comment on the structure of this expression: The prefactor $\gamma_{\mathbf{k}\sigma, \text{out}; \mathbf{k}\sigma, \text{in}}/\Gamma_{\mathbf{k}\sigma, \text{in}; \mathbf{k}\sigma, \text{in}}$ describes the probability that electrons excited above the vacuum energy actually leave the crystal. Photoemission is often described by a three-step picture [56–58]: First, electrons are excited, then they are transported to the surface, and finally they leave the crystal. In this work we are mainly interested in the first step. The second and third steps are incorporated phenomenologically by effective relaxation rates $\Gamma_{\mathbf{k}\sigma, \text{in}; \mathbf{k}\sigma, \text{in}}$, which describe electrons dropping below E_{vac} before they reach the surface, and effective transition rates $\gamma_{\mathbf{k}\sigma, \text{out}; \mathbf{k}\sigma, \text{in}}$ from states above E_{vac} within the solid to free electron states outside of the solid.

The total 2PPE yield consists of the three contributions

$$\mathcal{N}^{(4)} = \mathcal{N}_{\text{irr}}^{(4)} + \mathcal{N}_{\text{red}, 1}^{(4)} + \mathcal{N}_{\text{red}, 2}^{(4)} \quad (16)$$

corresponding to Fig. 7(a), (b), and (c), respectively. The second and third term rely on the nonlinear optical properties of the solid: The effective field \mathbf{E} leads to a second-order polarization $\mathbf{P}^{(2)}$, see Eq. (5), which is accompanied by an electric field $\mathbf{E}^{(2)}$. This field may lead to photoemission.

Since the diagram in Fig. 7(a) cannot be cut into two by severing a single photon line, the first term $\mathcal{N}_{\text{irr}}^{(4)}$ is irreducible, while the other two are reducible. The irreducible contribution in Eq. (16) can be written as

$$\mathcal{N}_{\text{irr}}^{(4)} = \int dt_1 dt_2 dt_3 dt_4 \eta_{ijkl}^{(4)}(t_1, t_2, t_3, t_4) \times E_i(t_1) E_j(t_2) E_k(t_3) E_l(t_4), \quad (17)$$

which is of *fourth* order in the electric field and of second order in the incoming intensity. Obviously, the structure of this expression is very similar to Eq. (7) for the SFG yield,

$$\mathcal{I}^{(2)} \propto \int dt dt_1 dt_2 dt_3 dt_4 \chi_{ijk}^{(2)}(t, t_1, t_2) \chi_{ilm}^{(2)}(t, t_3, t_4) \times E_j(t_1) E_k(t_2) E_l(t_3) E_m(t_4), \quad (18)$$

letting us expect similar interference effects in both cases. The other two contributions are

$$\mathcal{N}_{\text{red},1}^{(4)} = -4\pi \int dt_1 dt_2 dt_3 \eta_{ijk}^{(3)} \left[P_i^{(2)}(t_1) E_j(t_2) E_k(t_3) + E_i(t_1) P_j^{(2)}(t_2) E_k(t_3) + E_i(t_1) E_j(t_2) P_k^{(2)}(t_3) \right], \quad (19)$$

and

$$\mathcal{N}_{\text{red},2}^{(4)} = (4\pi)^2 \int dt_1 dt_2 \eta_{ij}^{(2)} P_i^{(2)}(t_1) P_j^{(2)}(t_2). \quad (20)$$

Since the nonlinear susceptibility $\chi^{(2)}$ contains three dipole matrix elements, the reducible contributions to the photoelectron current are of higher order in dipole matrix elements and are thus usually small. However, the nonlinear polarization $\mathbf{P}^{(2)}$ contains a factor of $\varepsilon_{\text{long}}^{-1}$. If the nonlinear polarization is enhanced due to a bulk plasma resonance at the sum frequency, one expects significant contributions from the reducible terms.

We next consider the response functions $\eta^{(n)}$ which determine the 2PPE yield $\mathcal{N}^{(4)}$. The functions $\eta^{(3)}$ and $\eta^{(4)}$ appearing in Eqs. (19) and (20), respectively, are of the same general form as $\eta^{(2)}$, Eq. (15), but have more terms resulting from different orders of the time arguments. Fully written out, the main, irreducible contribution to the 2PPE yield, Eq. (17), is

$$\mathcal{N}_{\text{irr}}^{(4)}(\mathbf{k}, \sigma) = \sum_{\mathbf{q}_1 \mathbf{q}_2 \mathbf{q}_3} \int dt_1 dt_2 dt_3 dt_4 \eta_{ijkl}^{(4)}(\mathbf{q}_1, \mathbf{q}_2, \mathbf{q}_3; t_1, t_2, t_3, t_4; \mathbf{k}, \sigma) E_i(\mathbf{q}_1, t_1) E_j(\mathbf{q}_2, t_2) \times E_k(\mathbf{q}_3, t_3) E_l(-\mathbf{q} - \mathbf{q}_1 - \mathbf{q}_2, t_4). \quad (21)$$

Defining the complex transition energy

$$\Omega_{\mathbf{k}_{\parallel} l; \mathbf{k}'_{\parallel} l'} \equiv \frac{E_{\mathbf{k}_{\parallel} l} - E_{\mathbf{k}'_{\parallel} l'}}{\hbar} - i\Gamma_{\mathbf{k}_{\parallel} l; \mathbf{k}'_{\parallel} l'}, \quad (22)$$

we obtain the response function

$$\begin{aligned} \eta_{ijkl}^{(4)}(\mathbf{q}_1, \mathbf{q}_2, \mathbf{q}_3; t_1, t_2, t_3, t_4; \mathbf{k}, \sigma) &= \frac{e^4}{\hbar^4} \frac{\gamma_{\mathbf{k}\sigma, \text{out}; \mathbf{k}\sigma, \text{in}}}{\Gamma_{\mathbf{k}\sigma, \text{in}; \mathbf{k}\sigma, \text{in}}} \sum_{\lambda_1 \lambda_2 \lambda_3} D_{\mathbf{k}\sigma, \text{in}; \mathbf{k}_{\parallel} + \mathbf{q}_{1\parallel}, \lambda_1}^i(\mathbf{q}_1) D_{\mathbf{k}_{\parallel} + \mathbf{q}_{1\parallel}, \lambda_1; \mathbf{k}_{\parallel} + \mathbf{q}_{1\parallel} + \mathbf{q}_{2\parallel}, \lambda_2}^j(\mathbf{q}_2) \\ &\times D_{\mathbf{k}_{\parallel} + \mathbf{q}_{1\parallel} + \mathbf{q}_{2\parallel}, \lambda_2; \mathbf{k}_{\parallel} + \mathbf{q}_{1\parallel} + \mathbf{q}_{2\parallel} + \mathbf{q}_{3\parallel}, \lambda_3}^k(\mathbf{q}_3) D_{\mathbf{k}_{\parallel} + \mathbf{q}_{1\parallel} + \mathbf{q}_{2\parallel} + \mathbf{q}_{3\parallel}, \lambda_3; \mathbf{k}\sigma, \text{in}}^l(-\mathbf{q}_1 - \mathbf{q}_2 - \mathbf{q}_3) \\ &\times \left\{ \Theta(t_1 - t_2) \Theta(t_2 - t_3) \Theta(t_3 - t_4) e^{-i\Omega_{\mathbf{k}_{\parallel} \lambda_1; \mathbf{k}\sigma, \text{in}}(t_1 - t_2)} e^{-i\Omega_{\mathbf{k}_{\parallel} \lambda_2; \mathbf{k}\sigma, \text{in}}(t_2 - t_3)} e^{-i\Omega_{\mathbf{k}_{\parallel} \lambda_3; \mathbf{k}\sigma, \text{in}}(t_3 - t_4)} [-f(E_{\mathbf{k}_{\parallel} \lambda_3})] \right. \\ &- \Theta(t_1 - t_2) \Theta(t_2 - t_4) \Theta(t_4 - t_3) e^{-i\Omega_{\mathbf{k}_{\parallel} \lambda_1; \mathbf{k}\sigma, \text{in}}(t_1 - t_2)} e^{-i\Omega_{\mathbf{k}_{\parallel} \lambda_2; \mathbf{k}\sigma, \text{in}}(t_2 - t_4)} e^{-i\Omega_{\mathbf{k}_{\parallel} \lambda_2; \mathbf{k}_{\parallel} \lambda_3}(t_4 - t_3)} [f(E_{\mathbf{k}_{\parallel} \lambda_3}) - f(E_{\mathbf{k}_{\parallel} \lambda_2})] \\ &\left. - \dots \right\}. \end{aligned} \quad (23)$$

There are eight terms in the curly braces, which correspond to different temporal orders of absorptions. See App. B for full results for $\eta^{(3)}$ and $\eta^{(4)}$.

Equation (23) forms the basis for our discussion of 2PPE. To clarify the time dependence exhibited in Eq. (23) we discuss the second term. The processes described by this term are illustrated in Fig. 8. The system starts out in equilibrium. The first absorption takes place at time t_3 and creates a superposition of the states $|\mathbf{k}_{\parallel}\lambda_2\rangle$ and $|\mathbf{k}_{\parallel}\lambda_3\rangle$, leading to oscillations at the frequency $(E_{\mathbf{k}_{\parallel}\lambda_3} - E_{\mathbf{k}_{\parallel}\lambda_2})/\hbar$ expressed by the third exponential factor in this term. The Fermi factors ensure that one of the states is initially occupied and the other is empty. Let us assume that $|\mathbf{k}_{\parallel}\lambda_2\rangle$ is occupied. The second absorption at t_4 changes the state into a superposition of $|\mathbf{k}_{\parallel}\lambda_2\rangle$ and the vacuum state $|\mathbf{k}\sigma, \text{in}\rangle$ and the third at t_2 changes it into a superposition of the vacuum state and $|\mathbf{k}_{\parallel}\lambda_1\rangle$. After the fourth absorption the electron is in a pure vacuum state and can leave the solid with finite probability. Of course, due to the sum over all bands there are usually several contributions of this type. Only if the superpositions decay very rapidly compared to the pure states, a description in terms of rate equations, as suggested by Fig. 2, is applicable [15,33,34]. Also compare the discussion of SFG above, see Fig. 4.

While SFG is only governed by the dephasing rates but not the energy relaxation rates, 2PPE depends on both. This is because in the 2PPE response function $\eta^{(4)}$ the change of occupation of states enters besides the polarization of the electron gas, whereas SFG only depends on the latter.

Note, the 2PPE yield contains *four* dipole matrix elements. Thus, even for inversion-symmetric crystals parity does not forbid 2PPE from the bulk. However, 2PPE is sensitive to a surface region of a thickness given by the mean free path of electrons above E_{vac} . The optical penetration depth is typically significantly larger than the mean free path and thus does not enter here. Equations (15) and (23) also illustrate that 2PPE is sensitive to specific points in the Brillouin zone: The photoelectron momentum \mathbf{k} measured by *momentum-resolved* 2PPE is approximately the same as the lattice momentum of the original unperturbed electron and also of the intermediate state due to the small photon momentum. These effects obviously require a theoretical description that considers the \mathbf{k} -dependent states in the solid, like our approach does, as opposed to both the random- \mathbf{k} approximation and Bloch equations. In view of the importance of angle-resolved (ordinary) photoemission spectroscopy (ARPES) for, *e.g.*, cuprate high- T_c superconductors, \mathbf{k} -resolved 2PPE is expected to yield interesting results in the future. On the other hand, if one only measures the total number of photoelectrons, the \mathbf{k} -space resolution is lost and 2PPE and SFG give very similar information.

Just as for SFG, the 2PPE response can also be written in frequency space,

$$\begin{aligned} \mathcal{N}_{\text{irr}}^{(4)} = & \int d\omega_1 d\omega_2 d\omega_3 \eta_{ijkl}^{(4)}(\omega_1, \omega_2, \omega_3) E_i(\omega_1) E_j(\omega_2) \\ & \times E_k(\omega_3) E_l(-\omega_1 - \omega_2 - \omega_3), \end{aligned} \quad (24)$$

etc. The Fourier-transformed response functions contain the same type of energy denominators as χ and $\chi^{(2)}$, showing that intermediate states are again virtual. On the other hand, the energy of the photoelectron is sharp, since it leaves the crystal and is thus in a *real* state.

The response expressions show that plasmons affect 2PPE in two ways: First, exactly like for SFG the effective field \mathbf{E} within the metal differs from the external field due to linear screening and is enhanced close to the plasmon resonance. Secondly, the reducible contributions in Eqs. (19) and (20) depend on the screened second-order polarization $\mathbf{P}^{(2)}$, which contains a factor of $\varepsilon_{\text{long}}^{-1}$, see Eq. (13). $\mathbf{P}^{(2)}$ is enhanced if the sum frequency is close to the plasmon frequency. In 2PPE this enhancement enters only in the reducible contributions of Eqs. (19) and (20). As discussed above, a plasma resonance can make these usually small contributions important.

III. DISCUSSION

The aim of the present section is to discuss and illustrate the results of the response theory for time-resolved SFG and 2PPE. In particular, we consider time-dependent effects on the femtosecond time scale. General statements can already be made without detailed knowledge of the response functions χ , $\chi^{(2)}$, and $\eta^{(n)}$. These results only depend on the response expressions for SFG and 2PPE, for example Eqs. (7) and (17), respectively, but not on the specific approximations made here.

The response expressions of the preceding section are valid for any time dependence of the exciting laser field. The time enters the response expressions for both SFG and 2PPE in two ways, apart from the step functions from causality, cf. Eqs. (10), (15), and (23): The difference between the time arguments of electric fields appears in exponentials oscillating at the transition frequency of the involved electron states and in exponentials decaying with the dephasing

rate of the superposition of the two states. (See the discussion of Figs. 4 and 8 for the interpretation of SFG and 2PPE in terms of electronic excitations.) Thus two absorptions will only lead to SFG or 2PPE if they take place within a time interval of the order of the relaxation time. The time passing between absorptions can be controlled by the pulse shape of the exciting laser pulses: Consider a pulse with possibly complicated envelope and total duration T . If T is much larger than typical relaxation times τ then the yield depends on the probability to absorb two photons within a time interval τ , which is independent of T . On the other hand, for $T \ll \tau$ there is almost no relaxation during the pulse. Thus τ can only be inferred from experiments if the total pulse duration is $T \sim \tau$.

To be more specific, in most experiments two approximately Gaussian pulses are used (pump-probe method) [1–16]. If the two pulses are of different mean frequencies ω_1 and ω_2 (two-color case) and one measures the SFG or 2PPE response at the sum frequency $\omega_1 + \omega_2$ then it is obvious which photon was absorbed out of which pulse. Then for long time delay ΔT compared to the single-pulse duration the relaxation rate of intermediate states can be read off directly from the ΔT dependence of the total yield. In pump-probe experiments with two pulses of the same mean frequency ω (single-color case), photons can be absorbed out of the same or different pulses. However, the contribution with all absorptions out of the same pulse obviously does not depend on ΔT , leading to a constant background. The remaining contribution again decays on the time scale τ . Note, in all these cases only a *typical* relaxation time enters, which usually is a weighted average over relaxation times of many states. If only a single relevant intermediate state is present, *e.g.*, for a quantum-well state, or if there are many but of similar relaxation rate, the relaxation time extracted from experiment will be the actual dephasing time of intermediate states. However, if intermediate states with very different dynamical properties are involved, for example if both *sp* and *d* bands are relevant, the measured relaxation time does not describe any single excited electron state.

In pump-probe SHG [1–5] or pump-probe single-color 2PPE [8,11–13,15] experiments, time-dependent interference effects are especially pronounced. Their origin is the following: The first absorption of a photon of frequency ω sets up an oscillating polarization. Now the probability of a second absorption depends on the relative phase of the oscillating polarization and the second photon. Since the oscillating polarization is described by the *off-diagonal* components of the density matrix ρ , a description in terms of rate equations, which omit them, is unable to describe interference.

For further illustration, we show results for SHG and 2PPE for a simple model. Unless stated otherwise, this model consists of three bands, the lowest one a three-dimensional tight-binding band 1 with band center at [59] -3.33 eV (all energies are measured relative to the Fermi energy) and half width 3.81 eV. The band maximum is at $\mathbf{k} = 0$. The second, rather flat tight-binding band 2 is centered at 2.29 eV with half width 0.48 eV and maximum also at $\mathbf{k} = 0$. Finally, there is a free electron band 3 representing electrons above the vacuum energy $E_{\text{vac}} = 4.29$ eV. We assume that the relaxation rates $\Gamma_{n_1 n_2}$ only depend on the band indices n_1, n_2 but not on the \mathbf{k} vector (see below). We use the energy relaxation rates $\hbar\Gamma_{22} = 0.191$ eV (corresponding to the lifetime $\tau_2 = 3.5$ fs) and $\hbar\Gamma_{33} = 0.381$ eV ($\tau_3 = 1.7$ fs) and no additional dephasing, *i.e.*, $\Gamma_{n_1, n_2}^{\text{ph}} = 0$ in Eq. (4). These short lifetimes are assumed to bring out the time-dependent effects more clearly. The dipole matrix elements are treated as constants. In the following we use this model to show how time-dependent effects emerge from our theory. For clarity, we neglect the Fresnel formulas in this part, which would only complicate the analysis without changing them qualitatively. We demonstrate that our theory gives reasonable results for a moderately complicated system. Obviously, it can be applied to a more realistic band structure at the expense of computation time. In addition, a realistic description of specific metals would require a proper treatment of the boundary conditions.

In Fig. 9(a) we show the 2PPE photoelectron yield for a particular momentum \mathbf{k} as a function of the delay time ΔT between two identical Gaussian pump and probe pulses. The mean wave length of the light is about $\lambda = 400$ nm, corresponding to a photon energy of $\hbar\omega = 3.05$ eV, and the duration of each pulse is 10.3 fs (full width at half maximum of the Gaussian envelope of the electric field). The vector \mathbf{k} is chosen so that the transition energies between the bands match $\hbar\omega$. In Fig. 9(b) we show the total SHG photon yield for exactly the same system. The signal is integrated over the whole Brillouin zone. The overall similarity of Figs. 9(a) and (b) demonstrates the similarity of the response expressions for SHG and 2PPE, compare Eqs. (7) and (17), for example. It means that similar information, *e.g.*, about the relaxation rates, can be obtained from both. The SHG curve is quite similar to the case of flat bands, shown in the inset in Fig. 9(b). This means that only a small region of \mathbf{k} space contributes. The resulting interference between different \mathbf{k} points becomes apparent in the tail of the interference pattern, where the main plot in Fig. 9(b) is more irregular and decays faster.

The 2PPE and SHG interference patterns in Fig. 9 show the well-known $8 : 1$ enhancement of the signal for $\Delta T = 0$. This enhancement is due to the yield being of fourth order in the field: For a single pulse the signal would be proportional to E^4 , for two isolated pulses this becomes $2E^4$, but for two overlapping pulses the amplitude is doubled, leading to $(2E)^4 = 16E^4$.

For both SHG and 2PPE, the central part of the interference pattern, which corresponds to short delay times ΔT up to about the single-pulse duration T , is dominated by the four-field autocorrelation function

$$\mathcal{A}_{ijkl}^{(4)}(\Delta T) \equiv \int d\omega_1 d\omega_2 d\omega_3 E_i(\omega_1) E_j(\omega_2) E_k(\omega_3) \times E_l(-\omega_1 - \omega_2 - \omega_3). \quad (25)$$

This part stems from the overlap of the two pulses and would be present even for very fast relaxation: Then the response functions $\chi^{(2)}$ and $\eta^{(4)}$ are very sharply peaked in time and thus nearly constant in frequency space, leading to $\mathcal{I}^{(2)} \propto \mathcal{A}^{(4)}$ and $\mathcal{N}_{\text{irr}}^{(4)} \propto \mathcal{A}^{(4)}$, for the SHG and 2PPE yield, respectively, see Eqs. (7) and (17). The autocorrelation signal alone is shown in Fig. 10(b).

In Sec. II we have discussed the response expressions for time-dependent SFG and 2PPE, (10) and (23), respectively. The first absorption creates an oscillating polarization. There is interference if the phase information is still preserved when the second photon is absorbed. This is governed by the dephasing time Γ_{21} . Thus the interference effects should decay with the time constant Γ_{21}^{-1} for large delays ΔT . This is shown in Fig. 10(a) for moderately fast ($\tau_2 = 6.9$ fs) and extremely fast ($\tau_2 = 0.86$ fs) relaxation. For the slower relaxation the tail indeed decays with Γ_{21}^{-1} but to observe this one obviously has to look at rather large ΔT , where the interference is already weak. For fast relaxation the curve is nearly indistinguishable from the autocorrelation in Fig. 10(b).

However, there is another crucial origin of the decay of interference: Intermediate states with energies that do not exactly match the energy of the original state plus the photon energy lead to *beatings* at the frequency of the detuning. This effect can be seen from the response expressions, as we now discuss for the case of SFG: For pulses of short duration T , the times t_1 and t_2 in Eq. (10) can be approximated by the pulse centers if we are interested in phenomena at frequencies small compared to T^{-1} . Then Eq. (10) shows that the polarization of the electron system shortly before the second absorption at t_1 is proportional to

$$\exp\left[i\frac{E_{\mathbf{k}_{\parallel}l} - E_{\mathbf{k}_{\parallel}l'}}{\hbar}(t_1 - t_2)\right] e^{-\Gamma_{\mathbf{k}_{\parallel}l'; \mathbf{k}_{\parallel}l}(t_1 - t_2)} e^{-i\omega t_2}, \quad (26)$$

omitting the sum over states. The last factor stems from the electric field of frequency ω describing the first absorption at time $t_2 < t_1$. The decaying exponential obviously describes the decay of interference with the dephasing rate $\Gamma_{\mathbf{k}_{\parallel}l'; \mathbf{k}_{\parallel}l}$. The oscillating terms are of the form $\exp[-i\delta\omega(t_1 - t_2)] \exp(-i\omega t_1)$ with $\delta\omega = (E_{\mathbf{k}_{\parallel}l'} - E_{\mathbf{k}_{\parallel}l})/\hbar - \omega$. Thus we expect slow beatings with the frequency $\delta\omega$, which lead to an initial decay of the signal on a time scale of $(\delta\omega)^{-1}$. There should be a recurring signal at large delay times, but this is in practice suppressed by relaxation. A similar argument can be made for 2PPE using Eq. (23). The effect is clearly seen in Fig. 11 for 2PPE: The width of the pattern is reduced by the detuning. Its tails also become more irregular.

Next, we turn to the effect of the band structure. We first discuss SHG. The SHG yield is determined by a sum over many transitions of different energies and dephasing rates, see Eq. (10). If the decay is governed by dephasing one observes the smallest dephasing rate at large time delays ΔT . However, at intermediate ΔT one sees an averaged rate. The dephasing rate $\Gamma_{\mathbf{k}_{\parallel}l; \mathbf{k}_{\parallel}l'}$ for two bands l and l' should usually not change dramatically with \mathbf{k} . On the other hand, the contribution of detuning is necessarily different for transitions with different transition frequencies. Thus, in the interference pattern a continuum of beating frequencies appears. Consequently, the initial decay is governed by an average detuning and later, probably unobservable, recurring signals are strongly reduced by destructive interference of different beating frequencies. The averages are weighted by a factor approximately inversely proportional to the detuning, as seen from Eq. (11). For narrow valence *and* intermediate state bands the average is restricted to a small effective band width W . For broader bands but constant relaxation rates throughout each band the dependence of numerical results (not shown) for the SHG yield on the width of the intermediate band turns out to be weak, since in this case all contributing processes are governed by the same relaxation rates [60]. Hence, if only a single intermediate state or a few states contribute significantly [39] or if there is a narrow band with uniform relaxation rates, the Bloch equations should work well. In this case our expressions reduce to a perturbative solution of the Bloch equations.

On the other hand, if there is strong electron-electron scattering at certain \mathbf{k} vectors, *e.g.*, due to Fermi surface nesting, the rates can be strongly \mathbf{k} dependent. If many states of different relaxation rates enter the SHG photon yield, then for broad bands the description of SHG using optical Bloch equations with a single intermediate state is not justified. If interference patterns are fitted with results from Bloch equations, there is no simple relation between the extracted relaxation rate and the dephasing rates of the excited electrons.

For 2PPE the situation is quite different, since this method allows to probe specific momenta \mathbf{k} in the Brillouin zone. Here, the band width is not crucial. There are typically several contributions to the photoelectron yield, since there are several unoccupied bands. The contributions are again weighted with the inverse detuning, but now there is only a small number of states involved for fixed photoelectron momentum \mathbf{k} . Thus a description in terms of a small number of states, *e.g.*, by optical Bloch equations, is valid. However, if one experimentally integrates over \mathbf{k} , 2PPE behaves much like SFG.

As mentioned above, 2PPE is, in principle, accompanied by SFG. It would be interesting to perform both SFG and 2PPE experiments on the same sample. The two techniques are complementary in that 2PPE gives information about specific points in the Brillouin zone whereas SFG averages over the whole zone. Furthermore, comparison of Eqs. (10) and (23) shows that while the general form of the expressions for SFG and 2PPE is similar, they do depend on the material parameters in quite different ways. We give three examples: First, 2PPE also depends on the energy relaxation rates (lifetimes) directly, where SFG only depends on the dephasing rates. Secondly, SFG crucially depends on the dipole matrix element \mathbf{D}_{31} of the transition from the excited state above E_{vac} to the original state in the Fermi sea, whereas 2PPE does not. Thus comparison of SFG and 2PPE may prove useful for measuring the dipole matrix elements. Thirdly, SFG generally results from a much thinner surface region than 2PPE and the relaxation rates obtained from 2PPE are more bulk-like, allowing to study the dependence of the rates on the distance from the surface. Finally, we have shown that there is a contribution to 2PPE from SFG light generated within the solid, see Eqs. (19) and (20) as well as Figs. 7(b) and (c). Simultaneous measurement of SFG and 2PPE may allow to detect this interesting effect.

Concerning the range of validity of the second-order response theory we remark the following. We consider first pump-probe SFG with a very long delay time ΔT . The first-order density operator $\rho^{(1)}$ describes the result of the first absorption. It contains a finite polarization (off-diagonal components) but no change of occupation (diagonal components), see Eq. (A4). A change of occupation is only obtained from $\rho^{(2)}$ and higher-order contributions, which involve a larger number of dipole matrix elements and are usually small compared to $\rho^{(1)}$. However, the off-diagonal components usually decay faster than the diagonal ones so that for long delay times the higher-order change of occupation can dominate over the second-order polarization and the second-order approximation breaks down. On the other hand, our expressions for 2PPE already include the change of occupation due to the first pulse, since we have directly calculated the photoelectron yield to fourth order. Thus the results should hold even for long delay times. For the case that the polarization has decayed at the time of the second pulse, but the non-equilibrium occupation has not, the resulting limiting form of $\eta^{(4)}$ is given by Eq. (B20). It only depends on the *energy relaxation* rates. This is the case where rate equations are appropriate [15,33,34]. Due to the vanishing polarization there are no interference effects.

There is an alternative and physically appealing description of pump-probe SFG and 2PPE as a *two-step process*: The first pulse creates a non-equilibrium distribution, which is probed by the second one. We now discuss the validity of calculations based on this picture. In App. A we derive an expression for the linear susceptibility of an electron gas in an arbitrary non-equilibrium state described by the density matrix ρ_{neq} , see Eq. (A12). If we insert $\rho^{(1)}$ due to the first pulse for ρ_{neq} , we obtain a two-step description for $\chi^{(2)}$ and the polarization $\mathbf{P}^{(2)}$. Omitting the details, we only state that the result is identical to the one obtained directly for the second-order polarization $\mathbf{P}^{(2)}$, Eq. (5), but with the full susceptibility $\chi^{(2)}$ replaced by its irreducible part $\chi_{\text{irr}}^{(2)}$ of Eq. (10). Thus, by assuming two separate absorptions and treating each in a first-order approximation, we lose the screening of the second-order polarization. This is not justified if the sum frequency lies close to the plasma resonance.

Next we consider a two-step description of 2PPE: The 2PPE photoelectron yield $\mathcal{N}^{(4)}$ is expressed in terms of an arbitrary non-equilibrium density matrix ρ_{neq} as discussed in App. B. Then the second-order density matrix $\rho^{(2)}$ due to the first pulse is inserted for ρ_{neq} . We reobtain the full irreducible fourth-order result $\mathcal{N}_{\text{irr}}^{(4)}$ of Fig. 7(a), but only part of the reducible contributions, Fig. 7(b), (c): The two-step description neglects contributions of two photons out of *different* pulses being converted into one SHG photon. These contributions may become important if the sum frequency is close to a plasma resonance. In conclusion, the two-step picture of SFG and 2PPE is valid unless the response at the sum frequency is enhanced by plasmon effects.

Finally, we emphasize that our theory can also describe time-resolved SFG and 2PPE from ferromagnetically ordered systems. Ultimately, the light couples to the (spin) magnetization through spin-orbit coupling, which is incorporated in the dipole matrix elements \mathbf{D} and the band structure. The spin-dependent matrix elements can be calculated by a perturbative expansion in the spin-orbit coupling [25,38]. SFG and 2PPE also depend on magnetic order through the spin-dependent band energies $E_{\mathbf{k}_{\parallel}l}$ and relaxation rates $\Gamma_{\mathbf{k}_{\parallel}l;\mathbf{k}'_{\parallel}l'}$. Of particular importance for magnetically-ordered materials is the rotation of the polarization of SHG light relative to incident light (NOLIMOKE) [25,38,39].

Compared to NOLIMOKE, 2PPE for magnetic systems has the advantage that in principle one can obtain information on the spin-dependent lifetimes of electrons in specific states $|\mathbf{k}_{\parallel}l\rangle$. In App. B we argue that for pump-probe experiments with long time delay ΔT the main contribution to 2PPE comes from the change of occupation brought about by the pump pulse. *Only* in this case the photoelectron yield is proportional to the occupation of the corresponding intermediate states. If in addition the matrix elements and the relaxation rates out of vacuum states depend only weakly on spin, then Eq. (B8) shows that the 2PPE yield becomes proportional to the transient magnetization in these intermediate states:

$$\mathcal{N}^{(4)}(\Delta T; \mathbf{k}, \sigma) \propto \rho_{\text{neq}; \mathbf{k}\nu\sigma; \mathbf{k}\nu\sigma}(\Delta T) = n_{\text{neq}; \mathbf{k}\nu\sigma}(\Delta T), \quad (27)$$

where $n_{\text{neq}; \mathbf{k}\nu\sigma}$ is the non-equilibrium occupation of the state $|\mathbf{k}\nu\sigma\rangle$ after the pump pulse (ν is a band index). Then $\mathcal{N}^{(4)}$ decays with the spin-dependent lifetime $\tau_{\mathbf{k}\nu\sigma}$.

In conclusion we have presented a unifying perturbative response theory for time-resolved SFG and 2PPE. The theory is fully quantum mechanical and contains the interference effects described by off-diagonal components of the density matrix. It does not rely on any assumption about the time or frequency dependence of the exciting laser pulses and works for any solid that can be described by a band structure, relaxation rates, and dipole matrix elements. We have only discussed metals but the response theory could also be applied to semiconductors and insulators. We have demonstrated that this theory is a suitable framework for the discussion of the time-dependent physics of SFG and 2PPE. We have shown that similar information as from 2PPE can be gained from SHG, which has been employed less often. Of course, 2PPE is sensitive to specific momenta \mathbf{k} in the Brillouin zone, while SHG in general is not. On the other hand, SHG is not restricted by the constraint $2\omega \geq E_{\text{vac}} - E_F$ of single-color 2PPE. A tight-binding model of a metal has been studied in order to show that the theory gives reasonable numerical results. The treatment of more realistic band structures is only a question of computation time. We have shown how relaxation rates and detuning affect the interference patterns in single-color pump-probe SHG and 2PPE experiments: The lifetime in the intermediate states and their detuning with respect to the photon energy lead to a similar narrowing of the interference patterns. Furthermore, we have discussed the role played by collective plasma excitations. Plasmon effects in both SFG and 2PPE can partly be understood in terms of field enhancement at the surface, but one also has to take the electric field accompanying a nonlinear polarization of the electron system into account.

ACKNOWLEDGMENTS

We thank Drs. W. Pfeiffer, G. Gerber, G. Bouzerar, and R. Knorren for valuable discussions. Financial support by the Deutsche Forschungsgemeinschaft through Sonderforschungsbereich 290 is gratefully acknowledged.

APPENDIX A: RESPONSE THEORY FOR THE NONLINEAR OPTICAL RESPONSE

In this appendix we derive the transverse second-order susceptibility and polarization for arbitrary pulse shapes of the exciting laser field. The resulting expressions allow to calculate the SFG yield for arbitrary pulse shapes, thereby going beyond the results of Hübner and Bennemann [25] for continuous-wave, monochromatic light. The self-consistent-field approach [24] is applied to a solid described by its band structure and relaxation rates. The flat surface is assumed to lie at $z = 0$ with the solid at $z < 0$.

The single-particle Hamiltonian is $H = H_0 + V$, where H_0 describes the unperturbed solid with the normalized eigenstates $|\mathbf{k}_{\parallel}l\rangle$ and eigenenergies $E_{\mathbf{k}_{\parallel}l}$. \mathbf{k}_{\parallel} is the momentum parallel to the surface and all other quantum numbers, discrete as well as continuous, are collectively denoted by l . The perturbation in the electric-dipole approximation [61, 21–23, 38–40, 46] is $V = -\mathbf{d} \cdot \mathbf{E}(\mathbf{r}, t) = +e\mathbf{r} \cdot \mathbf{E}(\mathbf{r}, t)$, where \mathbf{d} is the dipole operator and \mathbf{E} is the effective field within the solid, which is treated classically [62]. As noted above, the dipole approximation is justified since the skin depth is about one order of magnitude larger than the lattice constant so that the wave vector \mathbf{q} of the electromagnetic field is small.

The time evolution of the density operator ρ is described by the master or Liouville equation [49, 35]

$$\frac{d}{dt}\rho = \frac{1}{i\hbar} [H, \rho] + \mathcal{R}[\rho]. \quad (A1)$$

The linear functional $\mathcal{R}[\rho]$ is a formal representation of relaxation terms made explicit below. Matrix elements are written in the basis of Bloch states, $\rho_{\mathbf{k}_{\parallel}l; \mathbf{k}'_{\parallel}l'} \equiv \langle \mathbf{k}_{\parallel}l | \rho | \mathbf{k}'_{\parallel}l' \rangle$. The master equation then reads [35]

$$\begin{aligned} \frac{d}{dt}\rho_{\mathbf{k}_{\parallel}l; \mathbf{k}'_{\parallel}l'} &= \frac{1}{i\hbar} \langle \mathbf{k}_{\parallel}l | [H_0 + V, \rho] | \mathbf{k}'_{\parallel}l' \rangle + \delta_{\mathbf{k}_{\parallel}\mathbf{k}'_{\parallel}} \delta_{ll'} \\ &\times \sum'_{\mathbf{k}''l''} \gamma_{\mathbf{k}_{\parallel}l; \mathbf{k}''l''} \rho_{\mathbf{k}''l''; \mathbf{k}'_{\parallel}l'} - \Gamma_{\mathbf{k}_{\parallel}l; \mathbf{k}'_{\parallel}l'} \rho_{\mathbf{k}_{\parallel}l; \mathbf{k}'_{\parallel}l'}. \end{aligned} \quad (A2)$$

Here, $\Gamma_{\mathbf{k}_{\parallel}l;\mathbf{k}_{\parallel}l} \equiv \tau_{\mathbf{k}_{\parallel}l}^{-1}$ is the inverse lifetime of state $|\mathbf{k}_{\parallel}l\rangle$, which arises mainly from inelastic electron-electron scattering. $\gamma_{\mathbf{k}_{\parallel}l;\mathbf{k}'_{\parallel}l'}$ gives the rate of spontaneous transitions from state $|\mathbf{k}'_{\parallel}l'\rangle$ to state $|\mathbf{k}_{\parallel}l\rangle$. Because of conservation of electron number

$$\Gamma_{\mathbf{k}_{\parallel}l;\mathbf{k}_{\parallel}l} = \sum'_{\mathbf{k}'_{\parallel}l'} \gamma_{\mathbf{k}'_{\parallel}l';\mathbf{k}_{\parallel}l}. \quad (\text{A3})$$

Primed sums run over all states except $|\mathbf{k}_{\parallel}l\rangle$. $\Gamma_{\mathbf{k}_{\parallel}l;\mathbf{k}_{\parallel}l}$ and $\gamma_{\mathbf{k}_{\parallel}l;\mathbf{k}'_{\parallel}l'}$ describe *energy relaxation*, i.e., the change of the diagonal components of ρ , whereas the *dephasing* rate $\Gamma_{\mathbf{k}_{\parallel}l;\mathbf{k}'_{\parallel}l'}$ with $|\mathbf{k}_{\parallel}l\rangle \neq |\mathbf{k}'_{\parallel}l'\rangle$ describes relaxation of the off-diagonal components.

To solve the master equation (A2) perturbatively, the density operator is expanded in powers of the perturbation V as $\rho = \rho^{(0)} + \rho^{(1)} + \rho^{(2)} + \dots$. In thermal equilibrium the unperturbed density matrix can be expressed in terms of the Fermi function, $\rho_{\mathbf{k}_{\parallel}l;\mathbf{k}'_{\parallel}l'}^{(0)} = \delta_{\mathbf{k}_{\parallel}l;\mathbf{k}'_{\parallel}l'} \delta_{ll'} f(E_{\mathbf{k}_{\parallel}l})$. Inserting the Fourier transforms of the field \mathbf{E} and keeping only linear terms in Eq. (A2) one obtains the Fourier-transformed density matrix [63]

$$\begin{aligned} \rho_{\mathbf{k}_{\parallel}l;\mathbf{k}_{\parallel}+\mathbf{q}_{\parallel},l'}^{(1)}(\omega) &= e \sum_{q'_z} \mathbf{D}_{\mathbf{k}_{\parallel}l;\mathbf{k}_{\parallel}+\mathbf{q}_{\parallel},l'}(\mathbf{q}_{\parallel}, q'_z) \cdot \mathbf{E}(\mathbf{q}_{\parallel}, q'_z, \omega) \\ &\times \frac{f(E_{\mathbf{k}_{\parallel}+\mathbf{q}_{\parallel},l'}) - f(E_{\mathbf{k}_{\parallel}l})}{-\hbar\omega + E_{\mathbf{k}_{\parallel}+\mathbf{q}_{\parallel},l'} - E_{\mathbf{k}_{\parallel}l} - i\hbar\Gamma_{\mathbf{k}_{\parallel}l;\mathbf{k}_{\parallel}+\mathbf{q}_{\parallel},l'}}. \end{aligned} \quad (\text{A4})$$

Note that the diagonal components vanish: There is no change of occupation to first order. The dipole matrix elements are

$$\mathbf{D}_{\mathbf{k}_{\parallel}l;\mathbf{k}_{\parallel}+\mathbf{q}_{\parallel},l'}(\mathbf{q}_{\parallel}, q_z) \equiv \langle \mathbf{k}_{\parallel}l | \mathbf{r} e^{-i\mathbf{q}_{\parallel} \cdot \mathbf{r}_{\parallel}} e^{-iq_z z} | \mathbf{k}_{\parallel} + \mathbf{q}_{\parallel}, l' \rangle. \quad (\text{A5})$$

The polarization is given by the thermal average of the dipole operator,

$$\begin{aligned} \mathbf{P}(\mathbf{q}_{\parallel}, q_z, \omega) &= -\frac{e}{V} \text{Tr} \rho \mathbf{r} e^{i\mathbf{q} \cdot \mathbf{r}} \\ &= -\frac{e}{V} \sum_{\mathbf{k}_{\parallel}} \sum_{ll'} \rho_{\mathbf{k}_{\parallel}l;\mathbf{k}_{\parallel}+\mathbf{q}_{\parallel},l'}(\omega) \mathbf{D}_{\mathbf{k}_{\parallel}+\mathbf{q}_{\parallel},l';\mathbf{k}_{\parallel}l}(-\mathbf{q}), \end{aligned} \quad (\text{A6})$$

where V is the volume. This relation holds to all orders in V . To first order

$$P_i^{(1)}(\mathbf{q}_{\parallel}, q_z, \omega) = \sum_{q'_z} \chi_{ij}^{(1)}(\mathbf{q}_{\parallel}, q_z, q'_z, \omega) E_j(\mathbf{q}_{\parallel}, q'_z, \omega), \quad (\text{A7})$$

with the linear susceptibility of Lindhard form

$$\begin{aligned} \chi_{ij}^{(1)}(\mathbf{q}_{\parallel}, q_z, q'_z, \omega) &= -\frac{e^2}{V} \sum_{\mathbf{k}_{\parallel}} \sum_{ll'} D_{\mathbf{k}_{\parallel}+\mathbf{q}_{\parallel},l';\mathbf{k}_{\parallel}l}^i(-\mathbf{q}) \\ &\times D_{\mathbf{k}_{\parallel}l;\mathbf{k}_{\parallel}+\mathbf{q}_{\parallel},l'}^j(\mathbf{q}') \\ &\times \frac{f(E_{\mathbf{k}_{\parallel}+\mathbf{q}_{\parallel},l'}) - f(E_{\mathbf{k}_{\parallel}l})}{-\hbar\omega + E_{\mathbf{k}_{\parallel}+\mathbf{q}_{\parallel},l'} - E_{\mathbf{k}_{\parallel}l} - i\hbar\Gamma_{\mathbf{k}_{\parallel}l;\mathbf{k}_{\parallel}+\mathbf{q}_{\parallel},l'}}, \end{aligned} \quad (\text{A8})$$

shown diagrammatically in Fig. 3. It takes into account that the z component of momentum is not conserved.

From Eq. (A7) and Fourier transformation of Eq. (A8) one obtains the time-dependent result

$$\begin{aligned} P_i^{(1)}(\mathbf{q}_{\parallel}, q_z, t) &= \frac{1}{2\pi} \sum_{q'_z} \int_{-\infty}^{\infty} dt_1 \chi_{ij}(\mathbf{q}_{\parallel}, q_z, q'_z, t - t_1) \\ &\times E_j(\mathbf{q}_{\parallel}, q'_z, t_1), \end{aligned} \quad (\text{A9})$$

with

$$\begin{aligned}\chi_{ij}(\mathbf{q}_{\parallel}, q_z, q'_z; t - t_1) &= \frac{e^2}{V} \frac{2\pi i}{\hbar} \Theta(t - t_1) \sum_{\mathbf{k}_{\parallel}} \sum_{l'l''} D_{\mathbf{k}_{\parallel} + \mathbf{q}_{\parallel}, l'; \mathbf{k}_{\parallel} l}^i(-\mathbf{q}) D_{\mathbf{k}_{\parallel} l; \mathbf{k}_{\parallel} + \mathbf{q}_{\parallel}, l''}^j(\mathbf{q}') \\ &\times [f(E_{\mathbf{k}_{\parallel} + \mathbf{q}_{\parallel}, l'}) - f(E_{\mathbf{k}_{\parallel} l})] \exp\left[i \frac{E_{\mathbf{k}_{\parallel} + \mathbf{q}_{\parallel}, l'} - E_{\mathbf{k}_{\parallel} l}}{\hbar} (t - t_1)\right] \exp[-\Gamma_{\mathbf{k}_{\parallel} l; \mathbf{k}_{\parallel} + \mathbf{q}_{\parallel}, l'} (t - t_1)].\end{aligned}\quad (\text{A10})$$

The response is thus only non-zero if $t > t_1$, which expresses causality.

The above results have been obtained under the assumption that the system is initially in thermal equilibrium. We now temporarily drop this assumption. Then the unperturbed polarization $\mathbf{P}_{\text{neq}}^{(0)}$ is, in general, non-vanishing so that the electrons experience an effective field even in the absence of an external perturbation, leading to a master equation that is nonlinear in the non-equilibrium density operator $\rho_{\text{neq}}^{(0)}$. We assume, however, that this effect of electron-electron interaction is negligible. Then the linear response of a non-equilibrium system can be written as

$$P_{\text{neq};i}^{(1)}(\mathbf{q}_{\parallel}, q_z, \omega) = \sum_{\mathbf{q}'_{\parallel}, q'_z} \int_{-\infty}^{\infty} d\omega' \chi_{\text{neq};ij}^{(1)}(\mathbf{q}_{\parallel}, q_z, \omega; \mathbf{q}'_{\parallel}, q'_z, \omega') E_j(\mathbf{q}', \omega'), \quad (\text{A11})$$

with

$$\begin{aligned}\chi_{\text{neq};ij}^{(1)}(\mathbf{q}_{\parallel}, q_z, \omega; \mathbf{q}'_{\parallel}, q'_z, \omega') &= -\frac{e^2}{V} \sum_{\mathbf{k}_{\parallel}} \sum_{l'l''} D_{\mathbf{k}_{\parallel} + \mathbf{q}_{\parallel}, l'; \mathbf{k}_{\parallel} l}^i(-\mathbf{q}) \\ &\times \left[D_{\mathbf{k}_{\parallel} l; \mathbf{k}_{\parallel} + \mathbf{q}'_{\parallel}, l''}^j(\mathbf{q}') \rho_{\text{neq}; \mathbf{k}_{\parallel} + \mathbf{q}'_{\parallel}, l''; \mathbf{k}_{\parallel} + \mathbf{q}_{\parallel}, l'}^{(0)}(\omega - \omega') \right. \\ &\left. - \rho_{\text{neq}; \mathbf{k}_{\parallel} l; \mathbf{k}_{\parallel} + \mathbf{q}_{\parallel} - \mathbf{q}'_{\parallel}, l''}^{(0)}(\omega - \omega') D_{\mathbf{k}_{\parallel} + \mathbf{q}_{\parallel} - \mathbf{q}'_{\parallel}, l''; \mathbf{k}_{\parallel} + \mathbf{q}_{\parallel}, l'}^j(\mathbf{q}') \right].\end{aligned}\quad (\text{A12})$$

This equation gives the linear susceptibility in terms of an *arbitrary* density operator $\rho_{\text{neq}}^{(0)}$.

To return to the response of an equilibrium system, we now consider the second-order contribution. We collect the terms in the master equation (A2) that are of second order in the effective electric field. Thus,

$$\begin{aligned}\frac{d}{dt} \rho_{\mathbf{k}_{\parallel} l; \mathbf{k}_{\parallel} + \mathbf{q}_{\parallel}, l'}^{(2)} &= \frac{1}{i\hbar} (E_{\mathbf{k}_{\parallel} l} - E_{\mathbf{k}_{\parallel} + \mathbf{q}_{\parallel}, l'}) \rho_{\mathbf{k}_{\parallel} l; \mathbf{k}_{\parallel} + \mathbf{q}_{\parallel}, l'}^{(2)} \\ &+ \frac{1}{i\hbar} \langle \mathbf{k}_{\parallel} l | [V^{(1)}, \rho^{(1)}] | \mathbf{k}_{\parallel} + \mathbf{q}_{\parallel}, l' \rangle + \frac{1}{i\hbar} \langle \mathbf{k}_{\parallel} l | [V^{(2)}, \rho^{(0)}] | \mathbf{k}_{\parallel} + \mathbf{q}_{\parallel}, l' \rangle \\ &+ \delta_{\mathbf{q}_{\parallel} 0} \sum_{\mathbf{k}_{\parallel} l'}' \gamma_{\mathbf{k}_{\parallel} l; \mathbf{k}_{\parallel} \lambda} \rho_{\mathbf{k}_{\parallel} \lambda; \mathbf{k}_{\parallel} \lambda}^{(2)} - \Gamma_{\mathbf{k}_{\parallel} l; \mathbf{k}_{\parallel} + \mathbf{q}_{\parallel}, l'} \rho_{\mathbf{k}_{\parallel} l; \mathbf{k}_{\parallel} + \mathbf{q}_{\parallel}, l'}^{(2)}.\end{aligned}\quad (\text{A13})$$

$V^{(1)} \equiv V$ is the perturbation by the effective field. Higher-order perturbations $V^{(n)}$, $n \geq 2$, result from the electric field due to the displaced charge calculated at order n . From the expression for the electric field due to a polarization $\mathbf{P}^{(n)}$ [64],

$$E_i^{(n)}(\mathbf{r}) = \int d^3 r' \left[\frac{3(r_i - r'_i)(r_j - r'_j)}{|\mathbf{r} - \mathbf{r}'|^5} - \frac{1}{|\mathbf{r} - \mathbf{r}'|^3} - \frac{4\pi}{3} \delta(\mathbf{r} - \mathbf{r}') \right] P_j^{(n)}(\mathbf{r}'), \quad (\text{A14})$$

one obtains by Fourier transformation

$$\mathbf{E}^{(n)}(\mathbf{q}) = -4\pi \hat{\mathbf{q}} \hat{\mathbf{q}} \cdot \mathbf{P}^{(n)}(\mathbf{q}), \quad (\text{A15})$$

where $\hat{\mathbf{q}} \equiv \mathbf{q}/|\mathbf{q}|$. Thus only the longitudinal part of $\mathbf{P}^{(n)}$ leads to a higher-order perturbation

$$V^{(n)} = -\mathbf{d} \cdot \mathbf{E}^{(n)} = +e\mathbf{r} \cdot \mathbf{E}^{(n)}. \quad (\text{A16})$$

This is because only a longitudinal polarization leads to a non-zero polarization charge density. Note, due to the reduced symmetry at the surface a transverse electric field in general leads to a polarization with a longitudinal component.

From Eqs. (A6) and (A13) we then obtain for $\mathbf{q}_{\parallel} \neq 0$

$$\begin{aligned}
P_i^{(2)}(\mathbf{q}, \omega) = & -\frac{e^2}{V} \int d^2 k_{\parallel} \sum_{l'l''} \frac{D_{\mathbf{k}_{\parallel}+\mathbf{q}_{\parallel}, l'; \mathbf{k}_{\parallel} l}^i(-\mathbf{q})}{-\hbar\beta + E_{\mathbf{k}_{\parallel}+\mathbf{q}_{\parallel}, l'} - E_{\mathbf{k}_{\parallel} l} + i\Gamma_{\mathbf{k}_{\parallel} l; \mathbf{k}_{\parallel}+\mathbf{q}_{\parallel}, l'}} \\
& \times \int d^3 q' \sum_{\lambda} \int d\omega' \left[D_{\mathbf{k}_{\parallel} l; \mathbf{k}_{\parallel}+\mathbf{q}_{\parallel}, \lambda}^j(\mathbf{q}') \rho_{\mathbf{k}_{\parallel}+\mathbf{q}_{\parallel}, \lambda; \mathbf{k}_{\parallel}+\mathbf{q}_{\parallel}, l'}^{(1)}(\omega - \omega') \right. \\
& \quad \left. - \rho_{\mathbf{k}_{\parallel} l; \mathbf{k}_{\parallel}+\mathbf{q}_{\parallel}-\mathbf{q}_{\parallel}', \lambda}^{(1)}(\omega - \omega') D_{\mathbf{k}_{\parallel}+\mathbf{q}_{\parallel}-\mathbf{q}_{\parallel}', \lambda; \mathbf{k}_{\parallel}+\mathbf{q}_{\parallel}, l'}^j(\mathbf{q}') \right] E_j(\mathbf{q}', \omega') \\
& + 4\pi [f(E_{\mathbf{k}_{\parallel}+\mathbf{q}_{\parallel}, l'}) - f(E_{\mathbf{k}_{\parallel} l})] \int dq'_z D_{\mathbf{k}_{\parallel} l; \mathbf{k}_{\parallel}+\mathbf{q}_{\parallel}, l'}^j(\mathbf{q}') \hat{q}_j \hat{q}_k P_k^{(2)}(\mathbf{q}', \omega), \tag{A17}
\end{aligned}$$

where in the last term $\mathbf{q}'_{\parallel} = \mathbf{q}_{\parallel}$. The solution for $\mathbf{P}^{(2)}$ can be written as

$$P_i^{(2)}(\mathbf{q}, \omega) = \sum_{\mathbf{q}', \mathbf{q}''} \int_{-\infty}^{\infty} d\omega' \chi_{ijk}^{(2)}(\mathbf{q}, \mathbf{q}'; \omega, \omega') E_j(\mathbf{q}', \omega') E_k(\mathbf{q} - \mathbf{q}', \omega - \omega'), \tag{A18}$$

with the second-order susceptibility

$$\chi_{ijk}^{(2)}(\mathbf{q}, \mathbf{q}', \mathbf{q}''; \omega, \omega') = \sum_m \sum_{\kappa_z} \varepsilon_{\text{long}; \text{im}}^{-1}(\mathbf{q}_{\parallel}, q_z, \kappa_z, \omega) \chi_{\text{irr}; \text{mj}k}^{(2)}((\mathbf{q}_{\parallel}, \kappa_z), \mathbf{q}', \mathbf{q}''; \omega, \omega') \tag{A19}$$

and

$$\varepsilon_{\text{long}; \text{ij}}(\mathbf{q}_{\parallel}, q_z, \kappa_z, \omega) \equiv \varepsilon_{ik}(\mathbf{q}_{\parallel}, q_z, \kappa_z, \omega) \frac{(\mathbf{q}_{\parallel}, \kappa_z)_k (\mathbf{q}_{\parallel}, \kappa_z)_j}{\mathbf{q}_{\parallel} \cdot \mathbf{q}_{\parallel} + \kappa_z^2} \tag{A20}$$

and $\varepsilon = 1 + 4\pi\chi^{(1)}$ is the dielectric tensor. This expression means that $\varepsilon_{\text{long}}$ only acts on the longitudinal component. Note, $\varepsilon_{\text{long}; \text{ij}}^{-1}(\mathbf{q}_{\parallel}, q_z, \kappa_z, \omega)$ is the inverse matrix of $\varepsilon_{\text{long}}$ with respect to the indices (i, q_z) and (j, κ_z) .

The irreducible susceptibility in Eq. (A19) reads

$$\begin{aligned}
\chi_{\text{irr}; \text{ijk}}^{(2)}(\mathbf{q}, \mathbf{q}', \mathbf{q}''; \omega, \omega') = & -\frac{e^3}{V} \sum_{\mathbf{k}_{\parallel}} \sum_{l'l''} \frac{D_{\mathbf{k}_{\parallel}+\mathbf{q}_{\parallel}, l; \mathbf{k}_{\parallel} l''}^i(-\mathbf{q})}{-\hbar\omega + E_{\mathbf{k}_{\parallel}+\mathbf{q}_{\parallel}, l} - E_{\mathbf{k}_{\parallel} l''} - i\hbar\Gamma_{\mathbf{k}_{\parallel} l''; \mathbf{k}_{\parallel}+\mathbf{q}_{\parallel}, l}} \\
& \times \left[D_{\mathbf{k}_{\parallel} l''; \mathbf{k}_{\parallel}+\mathbf{q}_{\parallel}', l'}^j(\mathbf{q}') D_{\mathbf{k}_{\parallel}+\mathbf{q}_{\parallel}', l'; \mathbf{k}_{\parallel}+\mathbf{q}_{\parallel}, l}^k(\mathbf{q}'') \frac{f(E_{\mathbf{k}_{\parallel}+\mathbf{q}_{\parallel}, l}) - f(E_{\mathbf{k}_{\parallel}+\mathbf{q}_{\parallel}', l'})}{-\hbar\omega + \hbar\omega' + E_{\mathbf{k}_{\parallel}+\mathbf{q}_{\parallel}, l} - E_{\mathbf{k}_{\parallel}+\mathbf{q}_{\parallel}', l'} - i\hbar\Gamma_{\mathbf{k}_{\parallel}+\mathbf{q}_{\parallel}', l'; \mathbf{k}_{\parallel}+\mathbf{q}_{\parallel}, l}} \right. \\
& \quad \left. - D_{\mathbf{k}_{\parallel}+\mathbf{q}_{\parallel}-\mathbf{q}_{\parallel}', l'; \mathbf{k}_{\parallel}+\mathbf{q}_{\parallel}, l}^j(\mathbf{q}') D_{\mathbf{k}_{\parallel} l''; \mathbf{k}_{\parallel}+\mathbf{q}_{\parallel}-\mathbf{q}_{\parallel}', l'}^k(\mathbf{q}'') \frac{f(E_{\mathbf{k}_{\parallel}+\mathbf{q}_{\parallel}-\mathbf{q}_{\parallel}', l'}) - f(E_{\mathbf{k}_{\parallel} l''})}{-\hbar\omega + \hbar\omega' + E_{\mathbf{k}_{\parallel}+\mathbf{q}_{\parallel}-\mathbf{q}_{\parallel}', l'} - E_{\mathbf{k}_{\parallel} l''} - i\hbar\Gamma_{\mathbf{k}_{\parallel} l''; \mathbf{k}_{\parallel}+\mathbf{q}_{\parallel}-\mathbf{q}_{\parallel}', l'}} \right], \tag{A21}
\end{aligned}$$

shown diagrammatically in Fig. 5(a). The screening factor $\varepsilon_{\text{long}}^{-1}$ appearing in Eq. (A19) describes linear screening of the induced polarization. Finally, the time dependence of the polarization $\mathbf{P}^{(2)}$ is obtained by Fourier transformation of Eq. (A18) using Eq. (9), leading to Eq. (10).

APPENDIX B: RESPONSE THEORY FOR PHOTOEMISSION

In this appendix we give additional details of the derivation of the time-integrated photoelectron yield. We also present the analytical expressions for the response functions omitted in Sec. II B. The starting point is again the master equation (A1). The terms of order $n \geq 1$ can be calculated recursively,

$$\begin{aligned}
\frac{d}{dt} \rho_{\mathbf{k}_{\parallel} l; \mathbf{k}_{\parallel}+\mathbf{q}_{\parallel}, l'}^{(n)} = & \frac{1}{i\hbar} (E_{\mathbf{k}_{\parallel} l} - E_{\mathbf{k}_{\parallel}+\mathbf{q}_{\parallel}, l'}) \rho_{\mathbf{k}_{\parallel} l; \mathbf{k}_{\parallel}+\mathbf{q}_{\parallel}, l'}^{(n)} \\
& + \frac{1}{i\hbar} \sum_{m=1}^n \langle \mathbf{k}_{\parallel} l | [V^{(m)}, \rho^{(n-m)}] | \mathbf{k}_{\parallel} + \mathbf{q}_{\parallel}, l' \rangle \\
& + \delta_{\mathbf{q}_{\parallel} 0} \delta_{l'l'} \sum_{\kappa_{\parallel} \lambda} \gamma_{\mathbf{k}_{\parallel} l; \kappa_{\parallel} \lambda} \rho_{\kappa_{\parallel} \lambda; \kappa_{\parallel} \lambda}^{(n)} \\
& - \Gamma_{\mathbf{k}_{\parallel} l; \mathbf{k}_{\parallel}+\mathbf{q}_{\parallel}, l'} \rho_{\mathbf{k}_{\parallel} l; \mathbf{k}_{\parallel}+\mathbf{q}_{\parallel}, l'}^{(n)}. \tag{B1}
\end{aligned}$$

Here, $V^{(m)}$ is the perturbation of order m , see the discussion leading to Eq. (A16). Among the states $|\mathbf{k}_\parallel l\rangle$ etc. appearing in Eq. (B1) are states $|\mathbf{k}\sigma, \text{in}\rangle$ lying in the crystal above the vacuum level. We assume that electrons leaving the crystal are in states $|\mathbf{k}\sigma, \text{out}\rangle$ and are detected without further interaction and without returning to the solid. Then the only way their occupation can change is through spontaneous transitions out of $|\mathbf{k}\sigma, \text{in}\rangle$, governed by the rate $\gamma_{\mathbf{k}\sigma, \text{out}; \mathbf{k}\sigma, \text{in}}$. Note, in principle higher vacuum bands appear by shifting the (nearly) free electron dispersion back into the first Brillouin zone. We omit these bands for notational simplicity.

First, we consider the irreducible part $\rho_{\text{irr}}^{(n)}$. This is the contribution of only the direct, first-order perturbation $V^{(1)} = V$ at every step of the recursion. The resulting equation reads

$$\begin{aligned} \frac{d}{dt} \rho_{\text{irr}; \mathbf{k}_\parallel l; \mathbf{k}_\parallel + \mathbf{q}_\parallel, l'}^{(n)}(t) &= \frac{1}{i\hbar} (E_{\mathbf{k}_\parallel l} - E_{\mathbf{k}_\parallel + \mathbf{q}_\parallel, l'}) \rho_{\text{irr}; \mathbf{k}_\parallel l; \mathbf{k}_\parallel + \mathbf{q}_\parallel, l'}^{(n)}(t) \\ &+ \frac{e}{i\hbar} \sum_{\mathbf{q}'\lambda} \left[\mathbf{D}_{\mathbf{k}_\parallel l; \mathbf{k}_\parallel + \mathbf{q}'_\parallel, \lambda}(\mathbf{q}') \rho_{\text{irr}; \mathbf{k}_\parallel + \mathbf{q}'_\parallel, \lambda; \mathbf{k}_\parallel + \mathbf{q}_\parallel, l'}^{(n-1)}(t) - \rho_{\text{irr}; \mathbf{k}_\parallel l; \mathbf{k}_\parallel + \mathbf{q}_\parallel - \mathbf{q}'_\parallel, \lambda}^{(n-1)}(t) \mathbf{D}_{\mathbf{k}_\parallel + \mathbf{q}_\parallel - \mathbf{q}'_\parallel, \lambda; \mathbf{k}_\parallel + \mathbf{q}_\parallel, l'}(\mathbf{q}') \right] \cdot \mathbf{E}(\mathbf{q}', t) \\ &+ \delta_{\mathbf{q}_\parallel 0} \delta_{ll'} \sum_{\mathbf{\kappa}_\parallel \lambda}' \gamma_{\mathbf{k}_\parallel l; \mathbf{\kappa}_\parallel \lambda} \rho_{\text{irr}; \mathbf{\kappa}_\parallel \lambda; \mathbf{\kappa}_\parallel \lambda}^{(n)}(t) - \Gamma_{\mathbf{k}_\parallel l; \mathbf{k}_\parallel + \mathbf{q}_\parallel, l'} \rho_{\text{irr}; \mathbf{k}_\parallel l; \mathbf{k}_\parallel + \mathbf{q}_\parallel, l'}^{(n)}(t). \end{aligned} \quad (\text{B2})$$

In this and the following expressions we write the first sum in the form $\sum_{\mathbf{q}'\lambda}$ as a reminder that *all* components of the external momentum \mathbf{q}' are summed over. Hence, we here exclude q'_z from λ . The solution for the off-diagonal elements is

$$\begin{aligned} \rho_{\text{irr}; \mathbf{k}_\parallel l; \mathbf{k}_\parallel + \mathbf{q}_\parallel, l'}^{(n)}(t) &= \frac{e}{i\hbar} \int_{-\infty}^t dt_1 \sum_{\mathbf{q}'\lambda} e^{-\Gamma_{\mathbf{k}_\parallel l; \mathbf{k}_\parallel + \mathbf{q}_\parallel, l'}(t-t_1)} \exp\left[-i \frac{E_{\mathbf{k}_\parallel l} - E_{\mathbf{k}_\parallel + \mathbf{q}_\parallel, l'}}{\hbar} (t-t_1)\right] \\ &\times \left[\mathbf{D}_{\mathbf{k}_\parallel l; \mathbf{k}_\parallel + \mathbf{q}'_\parallel, \lambda}(\mathbf{q}') \rho_{\text{irr}; \mathbf{k}_\parallel + \mathbf{q}'_\parallel, \lambda; \mathbf{k}_\parallel + \mathbf{q}_\parallel, l'}^{(n-1)}(t_1) - \rho_{\text{irr}; \mathbf{k}_\parallel l; \mathbf{k}_\parallel + \mathbf{q}_\parallel - \mathbf{q}'_\parallel, \lambda}^{(n-1)}(t_1) \mathbf{D}_{\mathbf{k}_\parallel + \mathbf{q}_\parallel - \mathbf{q}'_\parallel, \lambda; \mathbf{k}_\parallel + \mathbf{q}_\parallel, l'}(\mathbf{q}') \right] \cdot \mathbf{E}(\mathbf{q}', t_1). \end{aligned} \quad (\text{B3})$$

For the diagonal components there is an additional contribution from the relaxation of secondary electrons into the given state out of higher-energy states [33,34], *i.e.*, the term with $\delta_{\mathbf{q}_\parallel 0} \delta_{ll'}$ in Eq. (B2). The diagonal components can be written in the implicit form

$$\begin{aligned} \rho_{\text{irr}; \mathbf{k}_\parallel l; \mathbf{k}_\parallel l}^{(n)}(t) &= \frac{e}{i\hbar} \int_{-\infty}^t dt_1 \sum_{\mathbf{q}'\lambda} e^{-\Gamma_{\mathbf{k}_\parallel l; \mathbf{k}_\parallel l}(t-t_1)} \left[\mathbf{D}_{\mathbf{k}_\parallel l; \mathbf{k}_\parallel + \mathbf{q}'_\parallel, \lambda}(\mathbf{q}') \rho_{\text{irr}; \mathbf{k}_\parallel + \mathbf{q}'_\parallel, \lambda; \mathbf{k}_\parallel l}^{(n-1)}(t_1) \right. \\ &\left. - \rho_{\text{irr}; \mathbf{k}_\parallel l; \mathbf{k}_\parallel - \mathbf{q}'_\parallel, \lambda}^{(n-1)}(t_1) \mathbf{D}_{\mathbf{k}_\parallel - \mathbf{q}'_\parallel, \lambda; \mathbf{k}_\parallel l}(\mathbf{q}') \right] \cdot \mathbf{E}(\mathbf{q}', t_1) + \int_{-\infty}^t dt_1 \sum_{\mathbf{\kappa}_\parallel \lambda}' \gamma_{\mathbf{k}_\parallel l; \mathbf{\kappa}_\parallel \lambda} \rho_{\text{irr}; \mathbf{\kappa}_\parallel \lambda; \mathbf{\kappa}_\parallel \lambda}^{(n)}(t_1). \end{aligned} \quad (\text{B4})$$

If the contribution of secondary electrons is small, Eq. (B3) describes *all* components.

The photoelectron yield for momentum \mathbf{k} and spin σ is given by the time integrated photoelectron current. Equivalently, it can be written as the occupation of the appropriate vacuum state,

$$\mathcal{N}(\mathbf{k}, \sigma) = \rho_{\mathbf{k}\sigma, \text{out}; \mathbf{k}\sigma, \text{out}}(t \rightarrow \infty), \quad (\text{B5})$$

since electrons are assumed not to leave the states $|\mathbf{k}\sigma, \text{out}\rangle$ again. For the electron states outside of the crystal

$$\frac{d}{dt} \rho_{\mathbf{k}\sigma, \text{out}; \mathbf{k}\sigma, \text{out}} = \gamma_{\mathbf{k}\sigma, \text{out}; \mathbf{k}\sigma, \text{in}} \rho_{\mathbf{k}\sigma, \text{in}; \mathbf{k}\sigma, \text{in}}, \quad (\text{B6})$$

since their occupation can only change due to electrons leaving the crystal. With Eq. (B5) we find

$$\mathcal{N}(\mathbf{k}, \sigma) = \gamma_{\mathbf{k}\sigma, \text{out}; \mathbf{k}\sigma, \text{in}} \int_{-\infty}^{\infty} dt \rho_{\mathbf{k}\sigma, \text{in}; \mathbf{k}\sigma, \text{in}}(t). \quad (\text{B7})$$

The irreducible contribution to order n is obtained by inserting the irreducible part of $\rho^{(n)}$, Eq. (B4), into this equation. After changing the order of integrals we obtain

$$\begin{aligned} \mathcal{N}_{\text{irr}}^{(n)}(\mathbf{k}, \sigma) &= \frac{e}{i\hbar} \frac{\gamma_{\mathbf{k}\sigma, \text{out}; \mathbf{k}\sigma, \text{in}}}{\Gamma_{\mathbf{k}\sigma, \text{in}; \mathbf{k}\sigma, \text{in}}} \int_{-\infty}^{\infty} dt \sum_{\mathbf{q}\lambda} \\ &\times \left[\mathbf{D}_{\mathbf{k}\sigma, \text{in}; \mathbf{k}_\parallel + \mathbf{q}_\parallel, \lambda}(\mathbf{q}) \rho_{\text{irr}; \mathbf{k}_\parallel + \mathbf{q}_\parallel, \lambda; \mathbf{k}\sigma, \text{in}}^{(n-1)}(t) \right. \\ &\left. - \rho_{\text{irr}; \mathbf{k}\sigma, \text{in}; \mathbf{k}_\parallel - \mathbf{q}_\parallel, \lambda}^{(n-1)}(t) \mathbf{D}_{\mathbf{k}_\parallel - \mathbf{q}_\parallel, \lambda; \mathbf{k}\sigma, \text{in}}(\mathbf{q}) \right] \cdot \mathbf{E}(\mathbf{q}, t), \end{aligned} \quad (\text{B8})$$

where we have used that there is no relaxation *into* the states above E_{vac} in the solid. Note, Eq. (B8) describes photoemission out of *any* (possibly non-equilibrium) state.

For ordinary photoemission, $\mathcal{N}^{(2)}$, we have to calculate the density operator to first order, $\rho^{(1)}$, which is purely irreducible. Consequently, the *full* ordinary photoelectron yield is obtained by inserting Eq. (B3) for $n = 1$ into Eq. (B8),

$$\begin{aligned} \mathcal{N}^{(2)}(\mathbf{k}, \sigma) &= \sum_{\mathbf{q}} \int dt_1 dt_2 E_i(\mathbf{q}, t_1) \\ &\quad \times \eta_{ij}^{(2)}(\mathbf{q}; t_1, t_2; \mathbf{k}, \sigma) E_j(-\mathbf{q}, t_2) \end{aligned} \quad (\text{B9})$$

with the response function

$$\begin{aligned} \eta_{ij}^{(2)}(\mathbf{q}; t_1, t_2; \mathbf{k}, \sigma) &= \frac{e^2}{\hbar^2} \frac{\gamma_{\mathbf{k}\sigma, \text{out}; \mathbf{k}\sigma, \text{in}}}{\Gamma_{\mathbf{k}\sigma, \text{in}; \mathbf{k}\sigma, \text{in}}} \sum_{\lambda} \\ &\quad \times D_{\mathbf{k}\sigma, \text{in}; \mathbf{k}_{\parallel} + \mathbf{q}_{\parallel}, \lambda}^i(\mathbf{q}) \exp \left[i \frac{E_{\mathbf{k}_{\parallel} + \mathbf{q}_{\parallel}, \lambda} - E_{\mathbf{k}\sigma, \text{in}}}{\hbar} (t_2 - t_1) \right] \\ &\quad \times e^{-\Gamma_{\mathbf{k}_{\parallel} + \mathbf{q}_{\parallel}, \lambda; \mathbf{k}\sigma, \text{in}} |t_2 - t_1|} f(E_{\mathbf{k}_{\parallel} + \mathbf{q}_{\parallel}, \lambda}) \\ &\quad \times D_{\mathbf{k}_{\parallel} + \mathbf{q}_{\parallel}, \lambda; \mathbf{k}\sigma, \text{in}}^j(-\mathbf{q}). \end{aligned} \quad (\text{B10})$$

Of course, all our results can also be written in the frequency domain. For ordinary photoemission this yields

$$\begin{aligned} \mathcal{N}^{(2)}(\mathbf{k}, \sigma) &= \sum_{\mathbf{q}} \int_{-\infty}^{\infty} d\omega E_i(\mathbf{q}, \omega) \\ &\quad \times \eta_{ij}^{(2)}(\mathbf{q}, \omega; \mathbf{k}, \sigma) E_j(-\mathbf{q}, -\omega) \end{aligned} \quad (\text{B11})$$

with

$$\begin{aligned} \eta_{ij}^{(2)}(\mathbf{q}, \omega; \mathbf{k}, \sigma) &= \frac{2\pi i e^2}{\hbar} \frac{\gamma_{\mathbf{k}\sigma, \text{out}; \mathbf{k}\sigma, \text{in}}}{\Gamma_{\mathbf{k}\sigma, \text{in}; \mathbf{k}\sigma, \text{in}}} \\ &\quad \times \sum_{\lambda} D_{\mathbf{k}\sigma, \text{in}; \mathbf{k}_{\parallel} + \mathbf{q}_{\parallel}, \lambda}^i(\mathbf{q}) \\ &\quad \times \left(\frac{1}{\hbar\omega + E_{\mathbf{k}_{\parallel} + \mathbf{q}_{\parallel}, \lambda} - E_{\mathbf{k}\sigma, \text{in}} + i\hbar\Gamma_{\mathbf{k}_{\parallel} + \mathbf{q}_{\parallel}, \lambda; \mathbf{k}\sigma, \text{in}}} \right. \\ &\quad \left. - \frac{1}{\hbar\omega + E_{\mathbf{k}_{\parallel} + \mathbf{q}_{\parallel}, \lambda} - E_{\mathbf{k}\sigma, \text{in}} - i\hbar\Gamma_{\mathbf{k}_{\parallel} + \mathbf{q}_{\parallel}, \lambda; \mathbf{k}\sigma, \text{in}}} \right) \\ &\quad \times f(E_{\mathbf{k}_{\parallel} + \mathbf{q}_{\parallel}, \lambda}) D_{\mathbf{k}_{\parallel} + \mathbf{q}_{\parallel}, \lambda; \mathbf{k}\sigma, \text{in}}^j(-\mathbf{q}). \end{aligned} \quad (\text{B12})$$

The third-order contribution, $\mathcal{N}^{(3)}$, is of interest since the irreducible third-order response appears in the reducible contributions to 2PPE. To calculate $\mathcal{N}_{\text{irr}}^{(3)}$ from Eq. (B8), we need the off-diagonal elements of $\rho_{\text{irr}}^{(2)}$ only, *i.e.*, the polarization of the electron system, which can be obtained from Eq. (B3) alone. The result is

$$\begin{aligned} \mathcal{N}_{\text{irr}}^{(3)}(\mathbf{k}, \sigma) &= \sum_{\mathbf{q}\mathbf{q}'} \int dt_1 dt_2 dt_3 \eta_{ijk}^{(3)}(\mathbf{q}, \mathbf{q}'; t_1, t_2, t_3; \mathbf{k}, \sigma) \\ &\quad \times E_i(\mathbf{q}, t_1) E_j(\mathbf{q}', t_2) E_k(-\mathbf{q} - \mathbf{q}', t_3) \end{aligned} \quad (\text{B13})$$

with

$$\begin{aligned} \eta_{ijk}^{(3)}(\mathbf{q}, \mathbf{q}'; t_1, t_2, t_3; \mathbf{k}, \sigma) &= \frac{ie^3}{\hbar^3} \frac{\gamma_{\mathbf{k}\sigma, \text{out}; \mathbf{k}\sigma, \text{in}}}{\Gamma_{\mathbf{k}\sigma, \text{in}; \mathbf{k}\sigma, \text{in}}} \sum_{\lambda\lambda'} D_{\mathbf{k}\sigma, \text{in}; \mathbf{k}_{\parallel} + \mathbf{q}_{\parallel}, \lambda}^i(\mathbf{q}) D_{\mathbf{k}_{\parallel} + \mathbf{q}_{\parallel}, \lambda; \mathbf{k}_{\parallel} + \mathbf{q}_{\parallel} + \mathbf{q}'_{\parallel}, \lambda'}^j(\mathbf{q}') D_{\mathbf{k}_{\parallel} + \mathbf{q}_{\parallel} + \mathbf{q}'_{\parallel}, \lambda'; \mathbf{k}\sigma, \text{in}}^k(-\mathbf{q} - \mathbf{q}') \\ &\quad \times \left(\Theta(t_1 - t_2) \Theta(t_2 - t_3) e^{-i\Omega_{\mathbf{k}_{\parallel} + \mathbf{q}_{\parallel}, \lambda; \mathbf{k}\sigma, \text{in}}(t_1 - t_2)} e^{-i\Omega_{\mathbf{k}_{\parallel} + \mathbf{q}_{\parallel} + \mathbf{q}'_{\parallel}, \lambda'; \mathbf{k}\sigma, \text{in}}(t_2 - t_3)} \left[-f(E_{\mathbf{k}_{\parallel} + \mathbf{q}_{\parallel} + \mathbf{q}'_{\parallel}, \lambda'}) \right] \right. \\ &\quad \left. - \Theta(t_1 - t_3) \Theta(t_3 - t_2) e^{-i\Omega_{\mathbf{k}_{\parallel} + \mathbf{q}_{\parallel}, \lambda; \mathbf{k}\sigma, \text{in}}(t_1 - t_3)} e^{-i\Omega_{\mathbf{k}_{\parallel} + \mathbf{q}_{\parallel}, \lambda; \mathbf{k}_{\parallel} + \mathbf{q}_{\parallel} + \mathbf{q}'_{\parallel}, \lambda'}(t_3 - t_2)} \left[f(E_{\mathbf{k}_{\parallel} + \mathbf{q}_{\parallel} + \mathbf{q}'_{\parallel}, \lambda'}) - f(E_{\mathbf{k}_{\parallel} + \mathbf{q}_{\parallel}, \lambda}) \right] \right) \end{aligned}$$

$$\begin{aligned}
& -\Theta(t_3 - t_1) \Theta(t_1 - t_2) e^{-i\Omega_{\mathbf{k}\sigma, \text{in}; \mathbf{k}_{\parallel} + \mathbf{q}_{\parallel} + \mathbf{q}'_{\parallel}, \lambda'}(t_3 - t_1)} e^{-i\Omega_{\mathbf{k}_{\parallel} + \mathbf{q}_{\parallel}, \lambda; \mathbf{k}_{\parallel} + \mathbf{q}_{\parallel} + \mathbf{q}'_{\parallel}, \lambda'}(t_1 - t_2)} \left[f(E_{\mathbf{k}_{\parallel} + \mathbf{q}_{\parallel} + \mathbf{q}'_{\parallel}, \lambda'}) - f(E_{\mathbf{k}_{\parallel} + \mathbf{q}_{\parallel}, \lambda}) \right] \\
& + \Theta(t_3 - t_2) \Theta(t_2 - t_1) e^{-i\Omega_{\mathbf{k}\sigma, \text{in}; \mathbf{k}_{\parallel} + \mathbf{q}_{\parallel} + \mathbf{q}'_{\parallel}, \lambda'}(t_3 - t_2)} e^{-i\Omega_{\mathbf{k}\sigma, \text{in}; \mathbf{k}_{\parallel} + \mathbf{q}_{\parallel}, \lambda}(t_2 - t_1)} f(E_{\mathbf{k}_{\parallel} + \mathbf{q}_{\parallel}, \lambda}).
\end{aligned} \tag{B14}$$

Here, $\Theta(t)$ is the step function and $\Omega_{\mathbf{k}l; \mathbf{k}'l'} \equiv (E_{\mathbf{k}l} - E_{\mathbf{k}'l'})/\hbar - i\Gamma_{\mathbf{k}l; \mathbf{k}'l'}$ is a complex transition frequency. The four terms in Eq. (B14) correspond to different time orders of photon absorptions. In itself, $\mathcal{N}^{(3)}$ is usually negligible compared to $\mathcal{N}^{(2)}$ for the following reasons: The three frequencies of incoming photons have to add up to zero so that one has to be the negative of the sum of the other two. However, then the sum frequency is already present in the exciting laser pulse and *ordinary* photoemission dominates the signal.

Finally, the irreducible contribution to fourth order has the general form

$$\begin{aligned}
\mathcal{N}_{\text{irr}}^{(4)}(\mathbf{k}, \sigma) &= \sum_{\mathbf{q}\mathbf{q}'\mathbf{q}''} \int dt_1 dt_2 dt_3 dt_4 \\
&\times \eta_{ijkl}^{(4)}(\mathbf{q}, \mathbf{q}', \mathbf{q}''; t_1, t_2, t_3, t_4; \mathbf{k}, \sigma) E_i(\mathbf{q}, t_1) E_j(\mathbf{q}', t_2) \\
&\times E_k(\mathbf{q}'', t_3) E_l(-\mathbf{q} - \mathbf{q}' - \mathbf{q}'', t_4).
\end{aligned} \tag{B15}$$

$\eta^{(4)}$ can be found by inserting Eqs. (B3) and (B4) into Eq. (B8). The photoelectron yield is determined by the off-diagonal components of $\rho^{(3)}$, which in turn depend on *all* components of $\rho^{(2)}$, including the diagonal ones. New physics enter here: The 2PPE current depends on both the polarization and the change of occupation to second order.

If the increase of the occupation due to secondary electrons is small to second order, we can use Eq. (B3) to calculate *all* components of $\rho^{(2)}$. The change of occupation due to dipole transitions and to relaxation *out of* excited states is included in Eq. (B3). Then the response function $\eta^{(4)}$ reads

$$\begin{aligned}
\eta_{ijkl}^{(4)}(\mathbf{q}, \mathbf{q}', \mathbf{q}''; t_1, t_2, t_3, t_4; \mathbf{k}, \sigma) &= \frac{e^4}{\hbar^4} \frac{\gamma_{\mathbf{k}\sigma, \text{out}; \mathbf{k}\sigma, \text{in}}}{\Gamma_{\mathbf{k}\sigma, \text{in}; \mathbf{k}\sigma, \text{in}}} \sum_{\lambda\lambda'\lambda''} D_{\mathbf{k}\sigma, \text{in}; \mathbf{k}_{\parallel} + \mathbf{q}_{\parallel}, \lambda}^i(\mathbf{q}) D_{\mathbf{k}_{\parallel} + \mathbf{q}_{\parallel}, \lambda; \mathbf{k}_{\parallel} + \mathbf{q}_{\parallel} + \mathbf{q}'_{\parallel}, \lambda'}^j(\mathbf{q}') \\
&\times D_{\mathbf{k}_{\parallel} + \mathbf{q}_{\parallel} + \mathbf{q}'_{\parallel}, \lambda'; \mathbf{k}_{\parallel} + \mathbf{q}_{\parallel} + \mathbf{q}'_{\parallel} + \mathbf{q}''_{\parallel}, \lambda''}^k(\mathbf{q}'') D_{\mathbf{k}_{\parallel} + \mathbf{q}_{\parallel} + \mathbf{q}'_{\parallel} + \mathbf{q}''_{\parallel}, \lambda''; \mathbf{k}\sigma, \text{in}}^l(-\mathbf{q} - \mathbf{q}' - \mathbf{q}'') \\
&\times \left[F(t_1 - t_2, t_2 - t_3, t_3 - t_4; 1, 0; 2, 0; 3, 0) - F(t_1 - t_2, t_2 - t_4, t_4 - t_3; 1, 0; 2, 0; 2, 3) \right. \\
&\quad - F(t_1 - t_4, t_4 - t_2, t_2 - t_3; 1, 0; 1, 3; 2, 3) + F(t_1 - t_4, t_4 - t_3, t_3 - t_2; 1, 0; 1, 3; 1, 2) \\
&\quad - F(t_4 - t_1, t_1 - t_2, t_2 - t_3; 0, 3; 1, 3; 2, 3) + F(t_4 - t_1, t_1 - t_3, t_3 - t_2; 0, 3; 1, 3; 1, 2) \\
&\quad \left. + F(t_4 - t_3, t_3 - t_1, t_1 - t_2; 0, 3; 0, 2; 1, 2) - F(t_4 - t_3, t_3 - t_2, t_2 - t_1; 0, 3; 0, 2; 0, 1) \right]
\end{aligned} \tag{B16}$$

with the auxilliary function

$$\begin{aligned}
F(\Delta t_1, \Delta t_2, \Delta t_3; n_1, n_2; n_3, n_4; n_5, n_6) &\equiv \Theta(\Delta t_1) \Theta(\Delta t_2) \Theta(\Delta t_3) \\
&\times e^{-i\Omega_{n_1, n_2} \Delta t_1} e^{-i\Omega_{n_3, n_4} \Delta t_2} e^{-i\Omega_{n_5, n_6} \Delta t_3} [f(E_{n_6}) - f(E_{n_5})],
\end{aligned} \tag{B17}$$

where the states $|n_i\rangle$ are defined as

$$\begin{aligned}
|0\rangle &\equiv |\mathbf{k}\sigma; \text{in}\rangle, & |1\rangle &\equiv |\mathbf{k}_{\parallel} + \mathbf{q}_{\parallel}, \lambda\rangle, \\
|2\rangle &\equiv |\mathbf{k}_{\parallel} + \mathbf{q}_{\parallel} + \mathbf{q}'_{\parallel}, \lambda'\rangle, & |3\rangle &\equiv |\mathbf{k}_{\parallel} + \mathbf{q}_{\parallel} + \mathbf{q}'_{\parallel} + \mathbf{q}''_{\parallel}, \lambda''\rangle.
\end{aligned} \tag{B18}$$

Thus the first term in the brackets in Eq. (B16) reads

$$\begin{aligned}
&\Theta(t - t_1) \Theta(t_1 - t_2) \Theta(t_2 - t_3) e^{-i\Omega_{\mathbf{k}_{\parallel} + \mathbf{q}_{\parallel}, \lambda; \mathbf{k}\sigma, \text{in}}(t - t_1)} e^{-i\Omega_{\mathbf{k}_{\parallel} + \mathbf{q}_{\parallel} + \mathbf{q}'_{\parallel}, \lambda'; \mathbf{k}\sigma, \text{in}}(t_1 - t_2)} \\
&\times e^{-i\Omega_{\mathbf{k}_{\parallel} + \mathbf{q}_{\parallel} + \mathbf{q}'_{\parallel} + \mathbf{q}''_{\parallel}, \lambda''; \mathbf{k}\sigma, \text{in}}(t_2 - t_3)} \underbrace{\left[f(E_{\mathbf{k}\sigma, \text{in}}) - f(E_{\mathbf{k}_{\parallel} + \mathbf{q}_{\parallel} + \mathbf{q}'_{\parallel} + \mathbf{q}''_{\parallel}, \lambda''}) \right]}_{=0}
\end{aligned} \tag{B19}$$

etc. $\eta^{(4)}$ has the same structure as $\eta^{(3)}$, only with more terms due to more possible time orders. One should exclude terms from Eq. (B16), specifically from the sum over bands, that correspond to processes for which the system returns to the equilibrium state after two of the four absorptions. These processes only contribute a small correction to the numerical prefactor of the ordinary photoelectron yield.

If, in addition, the typical time scale of the experiment, *e.g.*, the delay time in the pump-probe case, is long compared to the dephasing times, 2PPE can be described by the change of occupation alone. Interference effects are then absent. In this limit, only the terms F in Eq. (B16) with $n_3 = n_4$ contribute, where n_3 is an excited state reachable by a single absorption out of the Fermi sea. Then $\eta^{(4)}$ simplifies to

$$\begin{aligned} \eta_{ijkl}^{(4)}(\mathbf{q}, \mathbf{q}', \mathbf{q}''; t_1, t_2, t_3, t_4; \mathbf{k}, \sigma) &= \frac{e^4}{\hbar^4} \frac{\gamma_{\mathbf{k}\sigma, \text{out}; \mathbf{k}\sigma, \text{in}}}{\Gamma_{\mathbf{k}\sigma, \text{in}; \mathbf{k}\sigma, \text{in}}} \sum_{\lambda\lambda'} \\ &\times \delta_{\mathbf{q}' + \mathbf{q}''_0, 0} D_{\mathbf{k}\sigma, \text{in}; \mathbf{k}_{\parallel} + \mathbf{q}_{\parallel}, \lambda}^i(\mathbf{q}) D_{\mathbf{k}_{\parallel} + \mathbf{q}_{\parallel}, \lambda; \mathbf{k}_{\parallel} + \mathbf{q}_{\parallel} + \mathbf{q}'_{\parallel}, \lambda'}^j(\mathbf{q}') \\ &\times D_{\mathbf{k}_{\parallel} + \mathbf{q}_{\parallel} + \mathbf{q}'_{\parallel}, \lambda'; \mathbf{k}_{\parallel} + \mathbf{q}_{\parallel}, \lambda}^k(-\mathbf{q}') D_{\mathbf{k}_{\parallel} + \mathbf{q}_{\parallel}, \lambda; \mathbf{k}\sigma, \text{in}}^l(-\mathbf{q}) \\ &\times \left[-F(t_1 - t_4, t_4 - t_2, t_2 - t_3; 1, 0; 1, 1; 2, 1) \right. \\ &\quad + F(t_1 - t_4, t_4 - t_3, t_3 - t_2; 1, 0; 1, 1; 1, 2) \\ &\quad - F(t_4 - t_1, t_1 - t_2, t_2 - t_3; 0, 1; 1, 1; 2, 1) \\ &\quad \left. + F(t_4 - t_1, t_1 - t_3, t_3 - t_2; 0, 1; 1, 1; 1, 2) \right]. \end{aligned} \quad (\text{B20})$$

Note, $\eta^{(4)}$ is now proportional to $\exp(-\Gamma_{11}\Delta t)$ from the second exponential in Eq. (B17), where $\Gamma_{11} = \tau_1^{-1}$ is the *energy* relaxation rate of state $|1\rangle = |\mathbf{k}_{\parallel} + \mathbf{q}_{\parallel}, \lambda\rangle$ and Δt is the time between the second and third absorption. This is easy to understand: After the second absorption the electron is in the pure state $|1\rangle$, which decays with the rate Γ_{11} .

Reducible contributions to the photoelectron current result from nonlinear optical effects in the solid. They are obtained by replacing the effective electric field \mathbf{E} in Eqs. (B11) and (B13) by the electric field to second order, see Eq. (A15). For 2PPE we obtain the contributions given in Eqs. (19) and (20) and shown diagrammatically in Fig. 7(b) and (c). There are also contributions given by $\eta^{(2)}$ times a product of \mathbf{E} and the *third-order* polarization $\mathbf{P}^{(3)}$. These are only significant if the incident light contains a frequency component large enough to allow ordinary photoemission and we neglect them.

Finally, it is also possible to describe (ordinary) photoemission out of a general non-equilibrium state described by the density matrix ρ_{neq} . The irreducible contribution is obtained from Eq. (B8) for the photoelectron yield $\mathcal{N}^{(n)}$ by expressing $\rho_{\text{irr}}^{(n-1)}$ in terms of the lower-order $\rho_{\text{irr}}^{(n-2)}$ with the help of Eq. (B3). This is exact, since only off-diagonal components of $\rho_{\text{irr}}^{(n-1)}$ are needed. Then $\rho^{(n-2)}$ is replaced by ρ_{neq} . There is also a reducible part: Two photons can be converted into a single one at the sum frequency, which for non-equilibrium, when a finite polarization exists, can lead to a change of occupation of states above E_{vac} and thus to photoemission.

APPENDIX C: BOUNDARY EFFECTS

To express the effective electric field \mathbf{E} within the solid in terms of the applied laser field \mathbf{E}_{las} , as well as to relate the polarization \mathbf{P} of the electron system to the outgoing light \mathbf{E}_{out} , one has to take the proper boundary conditions at the surface into account. For completeness, we give the expressions for a perfectly flat surface of a non-magnetic medium assuming an isotropic dielectric function ε , following Refs. [20] and [21]. If the surface is perpendicular to the z direction and the plane of incidence corresponds to the xz plane the effective field within the solid is

$$\mathbf{E} = \begin{pmatrix} t_p f_c \cos \phi \\ t_s \sin \phi \\ t_p f_s \cos \phi \end{pmatrix} E_{\text{las}}, \quad (\text{C1})$$

where ϕ is the polarization angle. The incoming field is $(\cos \theta \cos \phi, \sin \phi, \sin \theta \cos \phi) E_{\text{las}}$, where θ is the angle of incidence. The projection coefficients f_s, f_c and transmission coefficients t_p, t_s are

$$f_s = \frac{\sin \theta}{n}, \quad f_c = \sqrt{1 - f_s^2}, \quad (\text{C2})$$

$$t_p = \frac{2 \cos \theta}{n \cos \theta + f_c}, \quad t_s = \frac{2 \cos \theta}{\cos \theta + n f_c}, \quad (\text{C3})$$

where $n = \sqrt{\varepsilon}$ is the refractive index. These equations are, of course, relevant for both SFG and 2PPE.

For the outgoing light, the electric field can be expressed in terms of the polarization [20,21]: Since we are interested in SFG from inversion-symmetric crystals, the second-order polarization $\mathbf{P}^{(2)}$ only has appreciable values in a thin surface layer of thickness λ_{SFG} (typically 2–3 monolayers). In the limit of small λ_{SFG} the outgoing electric field reads

$$\mathbf{E}_{\text{out}} = i \frac{\omega}{c} \lambda_{\text{SFG}} \begin{pmatrix} -\cos \Theta A_p [n^2 F_s P_z - F_c P_x] \\ A_s P_y \\ \sin \Theta A_p [n^2 F_s P_z - F_c P_x] \end{pmatrix}, \quad (\text{C4})$$

where Θ is the angle of emergence and

$$F_s = \frac{\sin \Theta}{n}, \quad F_c = \sqrt{1 - F_s^2}, \quad (\text{C5})$$

$$A_p = \frac{2\pi T_p}{\cos \Theta}, \quad A_s = \frac{2\pi T_s}{\cos \Theta}, \quad (\text{C6})$$

and the transmission coefficients are

$$T_p = \frac{2 \cos \Theta}{n \cos \Theta + F_c}, \quad T_s = \frac{2 \cos \Theta}{\cos \Theta + n F_c}. \quad (\text{C7})$$

Systems of several layers, such as the important case of a coupling prism separated from the metal by a thin layer of air (or vacuum) [65], can be described by *effective* Fresnel factors [66,67]. For magnetically ordered solids one can find similar expressions [67].

APPENDIX D: PLASMON EFFECTS

Since SFG and 2PPE may be strongly enhanced by collective plasma excitations, it is useful to discuss them in the framework of the response theory. Here, plasmons appear as superpositions of electric-field modes dressed with any number of electron-hole loops, represented by the Dyson equation shown in Fig. 5(b).

We have seen in Sec. II that in both SFG and 2PPE *bulk* plasmons essentially enter in two ways: The first is the *field enhancement* of the effective electric field \mathbf{E} described by the Fresnel formulas. This mechanism is relevant at the incident-light frequency. The second is the screening of the nonlinear polarization $\mathbf{P}^{(2)}$, which is caused by the effective electric field $\mathbf{E}^{(2)}$ accompanying this polarization and is relevant at the sum and difference frequencies. Note, in the case of pump-probe SFG with two pulses of different mean frequencies ω_1 and ω_2 , one of them *and* the sum frequency $\omega_1 + \omega_2$ can be close to the plasmon frequency. This so-called *double resonance* leads to a particularly strong enhancement [29].

Surface plasmons, on the other hand, are not as important in the case of a flat surface. One distinguishes monopole and higher multipole surface plasmons. In monopole modes the charge does not oscillate in the z direction [67,41]. They are characterized by a diverging reflectivity for p -polarized light, which requires $\varepsilon \leq -1$ and a complex angle of incidence θ . A complex θ cannot be achieved by plane waves so that these modes cannot be optically excited at a flat surface and thus do not enter in SFG and 2PPE. Deviations from perfect flatness or a coupling prism are required for such excitations [67,65]. The latter case can be studied in the framework of response theory by using effective Fresnel factors [67]. This works, since the RPA result for ε is sufficient for an approximate description of surface plasmons in non-magnetic materials [43,41,44]. Higher multipole modes oscillate out of the xy plane [41,68] and they do couple to the external field even for a flat surface [69]. These modes can also be described within the RPA, in principle [70,71,41]. At the frequencies of multipole modes one expects enhanced SFG and 2PPE yields. We do not discuss higher multipole modes further.

Next, we consider the decay of bulk plasmons. Their decay time is contained in the imaginary part of the dielectric function ε . Ultimately, any plasmon decays into a single particle-hole pair [72]. This process is described by Fig. 5(b), if the time runs to the *left*. The probability of this decay is determined by the phase space available for the final electron-hole pair. It is only energetically possible if the plasmon dispersion lies within the electron-hole continuum at the plasmon momentum \mathbf{q} , leading to hybridization of plasmon and electron-hole excitations and to Landau damping. On the other hand, decay into a single electron-hole pair may be possible close to the surface, since translational symmetry is broken and q_z is not conserved. If the energy of the electron is higher than the vacuum energy, photoemission may result. Creation of several pairs is possible by subsequent inelastic electron-electron scattering. A plasmon also loses energy through inelastic scattering of the virtual electrons and holes in the loop in Fig. 5(b). This process is governed

by the single-particle relaxation rates. The plasmon lifetime is thus shorter than typical lifetimes of the relevant excited electrons.

Since plasmons are bosons, any plasma mode can be multiply excited. In a recent experiment a single plasma mode of silver nanoparticles is excited twice, whereupon this double excitation decays into a *single* electron-hole pair with a certain probability [16,73]. This observation is easy to interpret in the present framework. 2PPE with the incident-light frequency close to the plasmon frequency is enhanced due to field enhancement. Since 2PPE is of fourth order in the effective field \mathbf{E} , it is much more strongly affected by the plasma resonance than ordinary photoemission. A plasmon ultimately decays into an electron-hole pair. The electron *can* then absorb another plasmon, without scattering first [72]. This process is just the reverse of the “coherent double-plasmon excitation” discussed in the literature [74,75]. The final energy of the electron-hole pair is twice the plasmon energy. If the electron energy lies above E_{vac} , 2PPE may result [16]. The general process is not specific to clusters but can also happen at flat surfaces, involving bulk plasmons. It would be interesting to look for this effect.

-
- [1] D. Steinmüller-Nethl, R.A. Höpfel, E. Gornik, A. Leitner, and F.R. Aussenegg, Phys. Rev. Lett. **68**, 389 (1992).
 - [2] J. Hohlfeld, E. Matthias, R. Knorren, and K.H. Bennemann, Phys. Rev. Lett. **78**, 4861 (1997); erratum **79**, 960 (1997).
 - [3] M. Simon, F. Träger, A. Assion, B. Lang, S. Voll, and G. Gerber, Chem. Phys. Lett. **296**, 579 (1998).
 - [4] J.-H. Klein-Wiele, P. Simon, and H.-G. Rubahn, Phys. Rev. Lett. **80**, 45 (1998).
 - [5] J. Güdde, U. Conrad, U. Jähnke, J. Hohlfeld, and E. Matthias, Phys. Rev. B **59**, R6608 (1999).
 - [6] R.W. Schoenlein, J.G. Fujimoto, G.L. Eesley, and T.W. Capehart, Phys. Rev. Lett. **61**, 2596 (1989); Phys. Rev. B **41**, 5436 (1990); *ibid.* **43**, 4688 (1991).
 - [7] C.A. Schmuttenmaer, M. Aeschlimann, H.E. Elsayed-Ali, R.J.D. Miller, D.A. Mantell, J. Cao, and Y. Gao, Phys. Rev. B **50**, 8957 (1994); S. Pawlik, M. Bauer, and M. Aeschlimann, Surf. Sci. **377-379**, 206 (1997).
 - [8] M. Aeschlimann, M. Bauer, and S. Pawlik, Chem. Phys. **205**, 127 (1996); M. Aeschlimann, M. Bauer, S. Pawlik, W. Weber, R. Burgermeister, D. Oberli, and H.C. Siegmann, Phys. Rev. Lett. **79**, 5158 (1997); M. Aeschlimann, R. Burgermeister, S. Pawlik, M. Bauer, D. Oberli, and W. Weber, J. Elec. Spectros. Relat. Phenom. **88-91**, 179 (1998).
 - [9] T. Hertel, E. Knoesel, M. Wolf, and G. Ertl, Phys. Rev. Lett. **76**, 535 (1996); M. Wolf, Surf. Sci. **377-379**, 343 (1997); T. Hertel, E. Knoesel, A. Hotzel, M. Wolf, and G. Ertl, J. Vac. Sci. Technol. A **15**, 1503 (1997); E. Knoesel, A. Hotzel, and M. Wolf, J. Electron Spectrosc. Relat. Phenom. **88-91**, 577 (1998).
 - [10] U. Höfer, I.L. Shumay, C. Reuß, U. Thomann, W. Wallauer, and T. Fauster, Science **277**, 1480 (1997).
 - [11] J. Cao, Y. Gao, R.J.D. Miller, H.E. Elsayed-Ali, and D.A. Mantell, Phys. Rev. B **56**, 1099 (1997).
 - [12] S. Ogawa, H. Nagano, H. Petek, and A.P. Heberle, Phys. Rev. Lett. **78**, 1339 (1997); H. Petek, A.P. Heberle, W. Nessler, H. Nagano, S. Kubota, N. Matsunami, N. Moriya, and S. Ogawa, Phys. Rev. Lett. **79**, 4649 (1997); H. Petek, H. Nagano, and S. Ogawa, Phys. Rev. Lett. **83**, 832 (1999); H. Petek, H. Nagano, M.J. Weida, and S. Ogawa, Chem. Phys. **251**, 71 (2000).
 - [13] E. Knoesel, A. Hotzel, and M. Wolf, Phys. Rev. B **57**, 12812 (1998).
 - [14] J. Lehmann, M. Merschdorf, A. Thon, S. Voll, and W. Pfeiffer, Phys. Rev. B **60**, 17037 (1999).
 - [15] R. Knorren, K.H. Bennemann, R. Burgermeister, and M. Aeschlimann, Phys. Rev. B **61**, 9427 (2000); M. Aeschlimann, M. Bauer, S. Pawlik, R. Knorren, G. Bouzerar, and K.H. Bennemann, Appl. Phys. A **71**, 485 (2000).
 - [16] K. Ertel, U. Kohl, J. Lehmann, M. Merschdorf, W. Pfeiffer, A. Thon, S. Voll, and G. Gerber, Appl. Phys. B **68**, 439 (1999); J. Lehmann, M. Merschdorf, W. Pfeiffer, A. Thon, S. Voll, and G. Gerber, J. Chem. Phys. **112**, 5428 (2000); M. Merschdorf, W. Pfeiffer, A. Thon, S. Voll, and G. Gerber, to be published in Appl. Phys. A; M. Merschdorf, W. Pfeiffer, A. Thon, S. Voll, and G. Gerber (unpublished).
 - [17] H. Petek and S. Ogawa, Prog. Surf. Sci. **56**, 239 (1997).
 - [18] *Femtosecond Technology*, edited by T. Kamiya, F. Saito, O. Wada, and H. Yajima (Springer, Berlin, 1999).
 - [19] R. Y. Shen, *Principles of Nonlinear Optics* (Wiley/Interscience, New York, 1984).
 - [20] J.E. Sipe, D.J. Moss, and H.M. van Driel, Phys. Rev. B **35**, 1129 (1987).
 - [21] W. Hübner, K.H. Bennemann, and K. Böhmer, Phys. Rev. B **50**, 17597 (1994).
 - [22] T.A. Luce, W. Hübner, and K.H. Bennemann, Z. Phys. B **102**, 223 (1997).
 - [23] T.A. Luce and K.H. Bennemann, Phys. Rev. B **58**, 15821 (1998).
 - [24] H. Ehrenreich and M.H. Cohen, Phys. Rev. **115**, 786 (1959).
 - [25] W. Hübner and K.H. Bennemann, Phys. Rev. B **40**, 5973 (1989).
 - [26] The dynamics on time scales longer than about 500 fs can be understood by assuming that the electrons have thermalized at an electronic temperature T_e . However, we are interested in faster effects here.
 - [27] A. Liebsch and W.L. Schaich, Phys. Rev. B **40**, 5401 (1989).

- [28] C.A. Ullrich, P.-G. Reinhard, and E. Suraud, J. Phys. B **30**, 5043 (1997).
- [29] A. Liebsch, Appl. Phys. B **68**, 301 (1999).
- [30] C. Kohl, E. Suraud, and P.-G. Reinhard, Europ. Phys. J. D **11**, 115 (2000).
- [31] W.-D. Schöne, R. Keyling, M. Bandic, and W. Ekardt, Phys. Rev. B **60**, 8616 (1999); R. Keyling, W.-D. Schöne, and W. Ekardt, Phys. Rev. B **61**, 1670 (2000).
- [32] I. Campillo, A. Rubio, J.M. Pitarke, A. Goldmann, and P.M. Echenique, Phys. Rev. Lett. **85**, 3241 (2000).
- [33] R. Knorren, G. Bouzerar, and K.H. Bennemann, Phys. Rev. B **63**, 094306 (2001).
- [34] R. Knorren, G. Bouzerar, and K.H. Bennemann, to be published in Phys. Rev. B, preprint cond-mat/0003305.
- [35] R. Loudon, *The quantum theory of light*, second edition (Clarendon Press, Oxford, 1983).
- [36] T.V. Shahbazyan and I.E. Perakis, Chem. Phys. **251**, 37 (2000).
- [37] K.-D. Tsuei, E.W. Plummer, A. Liebsch, K. Kempa, and P. Bakshi, Phys. Rev. Lett. **64**, 44 (1990); A. Liebsch, Phys. Rev. Lett. **71**, 145 (1993); H. Ishida and A. Liebsch, Phys. Rev. B **54**, 14127 (1996).
- [38] W. Hübner, Phys. Rev. B **42**, 11553 (1990); U. Pustogowa, W. Hübner, and K.H. Bennemann, Phys. Rev. B **48**, 8607 (1993); J.P. Dewitz and W. Hübner, Appl. Phys. B **68**, 491 (1999).
- [39] T.A. Luce, W. Hübner, and K.H. Bennemann, Phys. Rev. Lett. **77**, 2810 (1996).
- [40] T.A. Luce, W. Hübner, A. Kirilyuk, T. Rasing, and K.H. Bennemann, Phys. Rev. B **57**, 7377 (1998).
- [41] B.B. Dasgupta and D.E. Beck, in: *Electronic Surface Modes*, edited by A.D. Boardman (Wiley, Chichester, 1982), p. 77.
- [42] J. Lindhard, K. Dan. Vidensk. Selsk. Mat. Fys. Mett. **28**, 8 (1954).
- [43] J. Harris and A. Griffin, Can. J. Phys. **48**, 2592 (1970); Phys. Rev. B **3**, 749 (1971); Phys. Lett. **34A**, 51 (1971); *ibid.* **37A**, 387 (1971).
- [44] E.V. Chulkov, I. Sarria, V.M. Silkin, J.M. Pitarke, and P.M. Echenique, Phys. Rev. Lett. **80**, 4947 (1998).
- [45] G.D. Mahan, *Many-Particle Physics*, second edition (Plenum Press, New York, 1990).
- [46] V.M. Shalaev, C. Douketis, T. Haslett, T. Stuckless, and M. Moskovits, Phys. Rev. B **53**, 11193 (1996).
- [47] H. Ueba, Surf. Sci. **334**, L719 (1995).
- [48] For ways to go beyond the relaxation time approximation, see: I. E. Perakis and T. V. Shahbazyan, Surf. Sci. Rep. **40**, 1 (2000).
- [49] W.H. Louisell, *Quantum Statistical Properties of Radiation* (Wiley, New York, 1973).
- [50] The solid lines in the diagrams are to be understood as finite-temperature electronic Green functions that differ from the usual Matsubara Green functions by the phenomenological relaxation rates Γ .
- [51] If $|\mathbf{k}_{\parallel}l\rangle$ is a state in the Fermi sea then the first term in Eq. (10) corresponds to the process shown in Fig. 1(a), whereas in the second one an electron from deep below the Fermi energy is excited by the second absorption into the hole left by the first absorption.
- [52] Obviously the system could now emit a photon at the oscillation frequency. This is the linear optical response described by χ_{ij} .
- [53] The “simultaneous absorption” of two photons sometimes invoked in the interpretation of experiments does not have a physical meaning. The response is always integrated over *all* possible absorption times. Of course, there will only be a SFG or 2PPE signal if the time between two absorption is not much longer than typical relaxation times.
- [54] To obtain detailed quantitative agreement with experiment it may be necessary to use more advanced numerical calculations for ε in Eq. (13) [45,37].
- [55] R. Feder, in: *Polarized Electrons in Surface Physics*, edited by R. Feder (World Scientific, Singapore, 1985).
- [56] C.N. Bergland and W.E. Spicer, Phys. Rev. **136**, A1030 (1964); *ibid.* **136**, A1044 (1964).
- [57] B. Feuerbach, B. Fitton, and R.F. Willis, in *Photoemission and the Electronic Properties of Surfaces*, Ed. B. Feuerbach, B. Fitton, and R.F. Willis (Wiley, Chichester, 1978).
- [58] D.P. Woodruff and T.A. Delchar, *Modern techniques of surface science* (Cambridge University Press, Cambridge, 1986).
- [59] The fractional numerical parameter values result from restoration of units and are not in any way special.
- [60] For a significantly broader intermediate band the interference falls off slightly faster because processes with larger detuning obtain more weight relative to those with small detuning.
- [61] H. Haug and S.W. Koch, *Quantum Theory of the Optical and Electronic Properties of Semiconductors* (World Scientific, Singapore, 1990).
- [62] The dipole moment depends on the choice of origin. The correct choice satisfies $\mathbf{P} = 0$ in equilibrium, cf. Eq. (A6).
- [63] For the Fourier transformation we employ the conventions of Ref. [25].
- [64] J.D. Jackson, *Classical Electrodynamics*, 3rd edition (Wiley, New York, 1999).
- [65] A. Otto, Z. Phys. **216**, 398 (1968).
- [66] M. Born and E. Wolf, *Principles of Optics* (Pergamon Press, New York, 1975).
- [67] A.D. Boardman, in: *Electronic Surface Modes*, edited by A.D. Boardman (Wiley, Chichester, 1982), p. 1, and references therein.
- [68] However, if retardation is included, the relation between the multipole character and the density profile is not straightforward [76,67].
- [69] C. Schwartz and W.L. Schaich, J. Phys. C **17**, 537 (1984).
- [70] B.B. Dasgupta and A. Bagchi, Phys. Rev. B **19**, 4935 (1979).
- [71] A. Bagchi and A.K. Rajagopal, Solid State Commun. **31**, 127 (1979); A. Bagchi, R. Barrera, and A.K. Rajagopal, Phys.

Rev. B **20**, 4824 (1979).

[72] G.F. Bertsch, N. Van Giai, and N. Vinh Mau, Phys. Rev. A **61**, 033202 (2000).

[73] Although we treat a flat surface, the general physical picture applies to clusters as well. To treat clusters quantitatively in the present framework, one would have to insert the proper energy eigenstates in the response expressions.

[74] J.C. Ashley and R.H. Ritchie, Phys. Stat. Solidi **38**, 425 (1970).

[75] I. Campillo and J.M. Pitarke, Nucl. Instr. Meth. Phys. Res. B **115**, 75 (1996).

[76] A.D. Boardman, B.V. Paranjape, and Y.O. Nakamura, Phys. Stat. Sol. (b) **75**, 347 (1976).

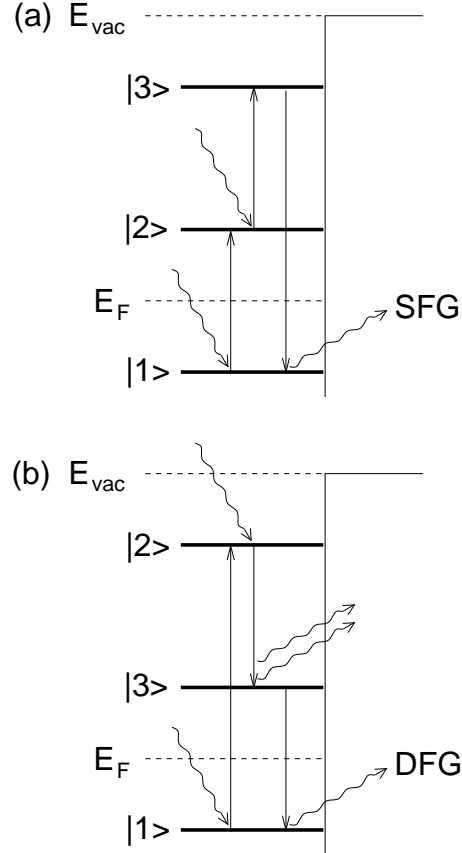


FIG. 1. Simplified representation of (a) sum-frequency generation (SFG) and (b) difference-frequency generation (DFG). E_F is the Fermi energy and E_{vac} is the vacuum energy. In SFG two photons of frequencies ω_1 and ω_2 are absorbed and a single photon of frequency $\omega_1 + \omega_2$ is emitted. In DFG a photon of frequency ω_1 is absorbed, a photon of frequency ω_2 leads to induced emission, and finally a photon of frequency $|\omega_1 - \omega_2|$ is emitted. The two photons may be provided by one or two laser pulses. A more careful analysis on the basis of response theory is given in Sec. II A.

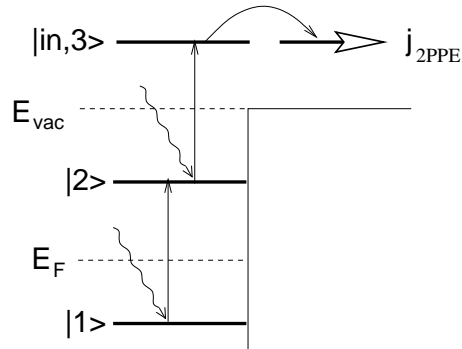


FIG. 2. Simplified representation of two-photon photoemission (2PPE), where E_F is the Fermi energy and E_{vac} the vacuum energy. The curved arrow denotes electrons leaving the crystal. Here, two photons of frequencies ω_1 and ω_2 (out of the same or different pulses) are absorbed. Compared to SFG, Fig. 1(a), the excitation energy is now so large that electrons are excited above E_{vac} and can leave the solid. Note, SFG is also possible.

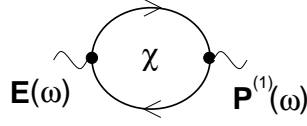


FIG. 3. The Feynman diagram for the linear susceptibility χ relating the linear polarization $\mathbf{P}^{(1)}$ to the effective electric field \mathbf{E} [50].

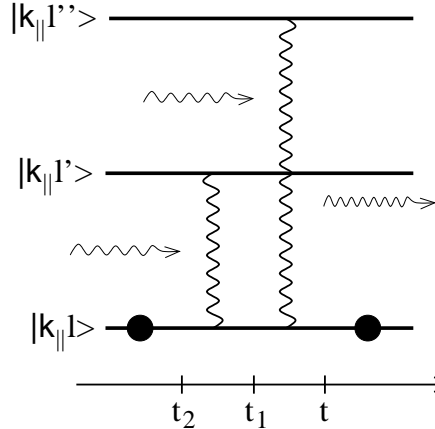


FIG. 4. Interpretation of a process contributing to SFG. An electron is excited from a pure state in the Fermi sea to a superposition by the absorption of two photons. It then return to the original pure state by emission of a SFG photon. The times of the absorptions and the emission are indicated. The heavy wavy lines here denote superpositions, while the black dots represent pure eigenstates.

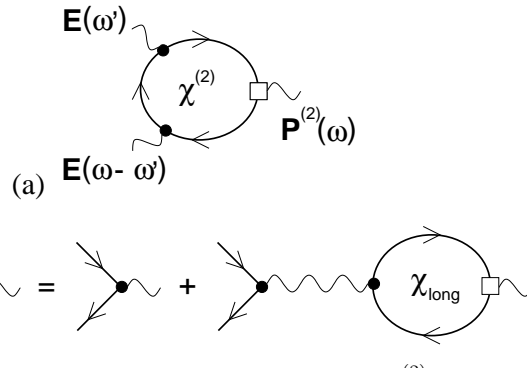


FIG. 5. (a) Diagrammatic representation of the second-order susceptibility $\chi^{(2)}$ in terms of the effective electric field \mathbf{E} . $\mathbf{P}^{(2)}$ is the induced nonlinear polarization. The square vertex represents the factor $\epsilon_{\text{long}}^{-1}$ at the frequency of $\mathbf{P}^{(2)}$. It appears if one self-consistently takes into account the electric field due to the polarization of the electron system and is given by the Dyson equation shown in (b). Note, χ_{long} only acts on the longitudinal field components, see text. The factor $\epsilon_{\text{long}}^{-1}$ can be enhanced by the plasma resonance.

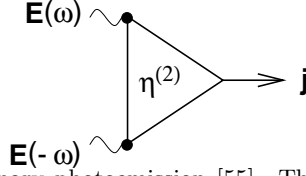


FIG. 6. Diagrammatic representation of ordinary photoemission [55]. The wavy lines denote the effective electric field \mathbf{E} within the solid and the arrow denotes the emitted electron current \mathbf{j} (or the photoelectron yield), which is of second order in the electric field. The response function $\eta^{(2)}$ is discussed in the text.

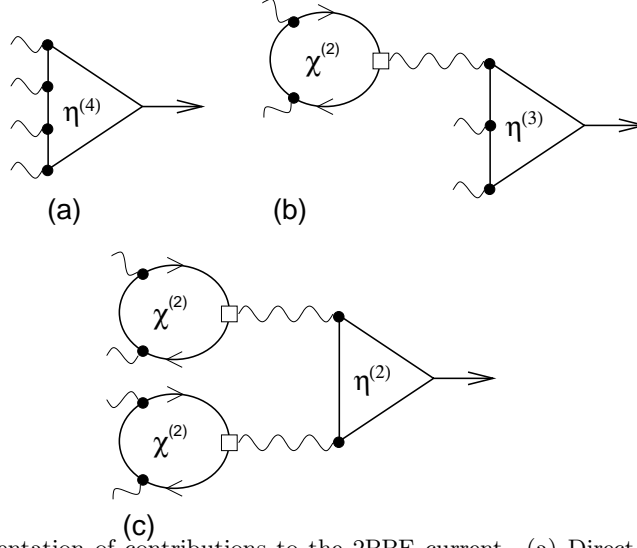


FIG. 7. Diagrammatic representation of contributions to the 2PPE current. (a) Direct irreducible contribution involving four transitions induced by the effective electric field \mathbf{E} . (b) Reducible process involving conversion of two photons to a SHG photon and subsequent photoemission of third order in the fields. (c) Reducible process involving conversion of all four photons to two SHG photons and ordinary photoemission (of second order in the fields) induced by the SHG light. The square vertex, representing a factor of $\varepsilon_{\text{long}}^{-1}$, is defined in Fig. 5(b). Plasma excitations again enter through this vertex.

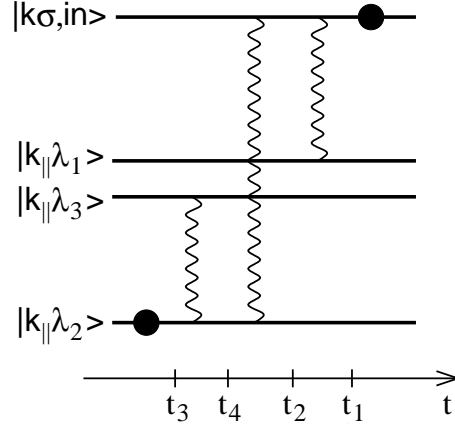


FIG. 8. Interpretation of one of the processes contributing to 2PPE. An electron is excited from a pure state in the Fermi sea to a pure vacuum state by absorption of four photons. The times t_i of the absorptions are indicated (the photons are not drawn in for clarity). The heavy wavy lines denote superpositions, while the black dots represent pure eigenstates. Compare Fig. 4 for a corresponding illustration of SFG.

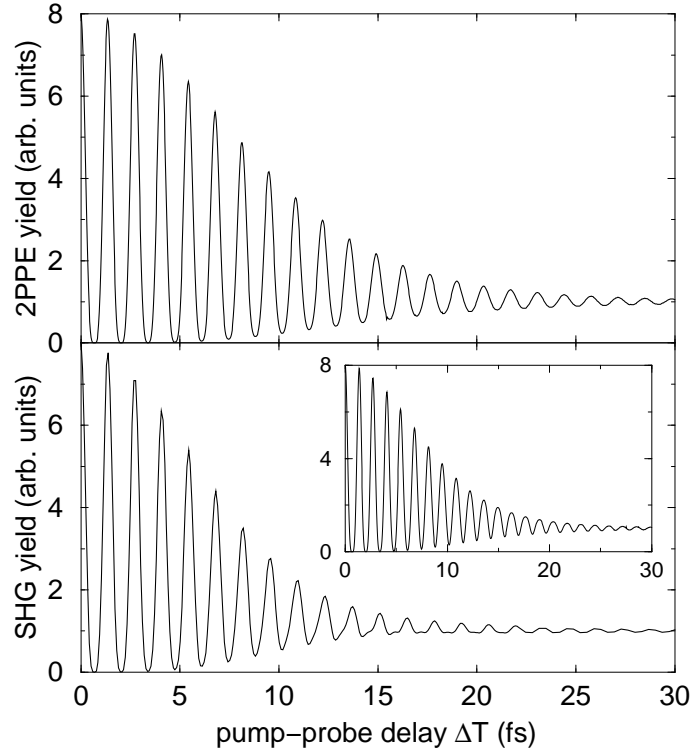


FIG. 9. (a) Total yield of photoelectrons of momentum \mathbf{k} for single-color pump-probe 2PPE as a function of the delay time ΔT . The parameters of the model are given in the text. The \mathbf{k} vector is chosen such that the transition frequencies perfectly match the frequency of incoming light. Only results for $\Delta T > 0$ are shown, since the curve is symmetric about $\Delta T = 0$ for identical pump and probe pulses. All curves in this and the following figures are scaled such that the limit for large ΔT is unity. (b) Total SHG yield for single-color pump-probe SHG as a function of the delay time ΔT using the same parameters. The inset shows the SHG yield for flat bands with transition frequencies that match the light frequency perfectly.

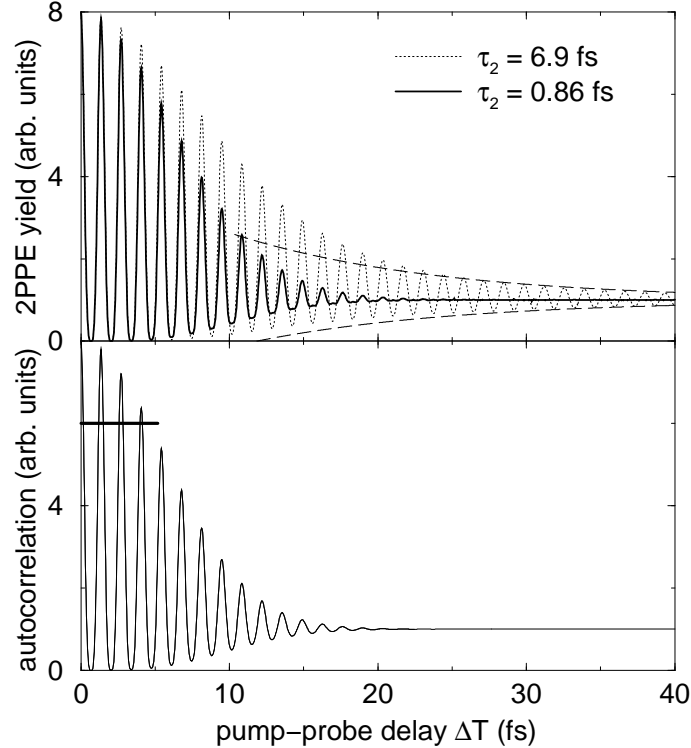


FIG. 10. Demonstration of the lifetime dependence of 2PPE. (a) Total 2PPE yield for the same model parameters as in Fig. 9 with a lifetime of the intermediate state of $\tau_2 = 6.9$ fs (dotted curve) and with the very small value $\tau_2 = 0.86$ fs (heavy solid curve). The dashed curves show the exponential decay with the dephasing rate $\Gamma_{12} = \tau_2^{-1}/2$ for $\tau_2 = 6.9$ fs. (b) Four-field autocorrelation function of the pump-probe laser field. Note the similarity to the fast-relaxation result in (a). The black bar denotes half the laser pulse duration.

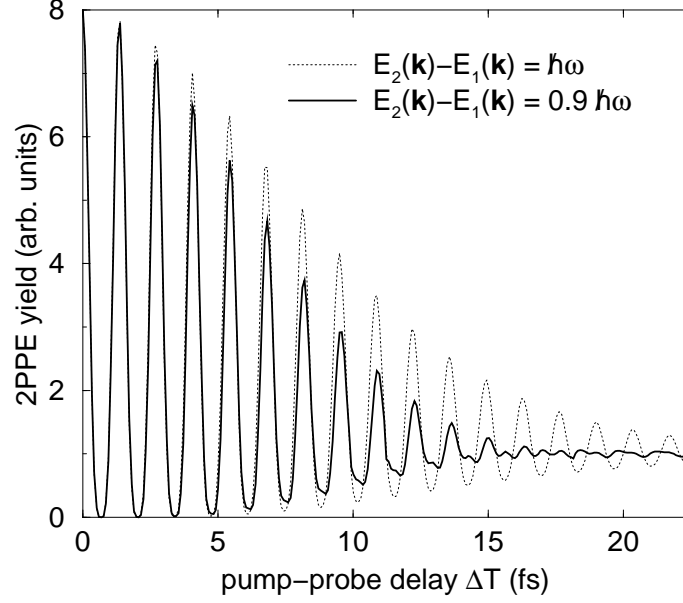


FIG. 11. Demonstration of the dependence of 2PPE on the detuning of the intermediate band. The heavy solid curve shows the total 2PPE yield for the same parameters as used in Fig. 9 but with the intermediate band shifted downward in energy by $0.1\hbar\omega$. ω is the mean frequency of the exciting laser field. For comparison, the dotted curve shows the 2PPE yield for unshifted bands.